Precambrian Research 354 (2021) 106060

Contents lists available at ScienceDirect

Precambrian Research

journal homepage: www.elsevier.com/locate/precamres

Pre-orogenic connection of the foreland domains of the Kaoko–Dom Feliciano–Gariep orogenic system

Jack James Percival [a,*], Jiří Konopásek [a,b], Ragnhild Eiesland [a], Jiří Sláma [c], Roberto Sacks de Campos [d], Matheus Ariel Battisti [e], Maria de Fátima Bitencourt [e]

[a] Department of Geosciences, UiT–The Arctic University of Norway, Dramsveien 201, 9037 Tromsø, Norway
[b] Czech Geological Survey, Klárov 3, 118 21 Prague 1, Czech Republic
[c] Institute of Geology of the Czech Academy of Sciences, Rozvojová 269, 165 00 Prague 6, Czech Republic
[d] Programa de Pós-graduação em Geologia (PPGGeologia), Universidade Federal de Santa Catarina (UFSC), Florianópolis, SC, Brazil
[e] Programa de Pós-graduação em Geociências, Instituto de Geociências, Universidade Federal do Rio Grande do Sul, Porto Alegre, Brazil

ARTICLE INFO

Keywords:
Gondwana
Rodinia
Dom Feliciano Belt
Kaoko Belt
Neoproterozoic
Rifting

ABSTRACT

Neoproterozoic metasedimentary rocks in the foreland domains of the Kaoko–Dom Feliciano–Gariep orogenic system record sedimentation from the breakup of Rodinia to the amalgamation of Gondwana, and thus provide ideal subjects for investigation of the mutual pre-orogenic positions of rifted margins of the African and South American cratonic blocks. U–Pb isotopic dating of zircon in the Brusque Complex of the northern Dom Feliciano Belt, Brazil, provides new constraints on the timing and sources of Neoproterozoic sedimentation along the eastern margin of the Luis Alves Craton. The minimum age of sedimentation is constrained by a U–Pb zircon age of 811 ± 6 Ma from a dyke cross-cutting the Brusque Complex. U–Pb detrital zircon analysis reveals two distinct groups: one with ages ca. 2.2–2.0 Ga consistent with erosion of the adjacent Luis Alves Craton, and another with ages ca. 2.1–1.8 and 1.6–1.0 Ga consistent with erosion of Paleoproterozoic to Mesoproterozoic igneous provinces and/or supracrustal sequences at the edge of the Congo Craton. The age distributions match with analogous rocks of the central Dom Feliciano Belt and the Kaoko Belt, and show similarities with the Gariep Belt, suggesting deposition in a system of coeval and spatially related paleobasins around the time of Rodinia breakup. The absence of Neoproterozoic detrital zircon close to the age of sedimentation suggests deposition in an intracontinental rift or passive margin. A third group contains a significant proportion of Neoproterozoic ca. 670–560 Ma zircon, suggesting similarities with the adjacent Itajaí Basin syn-orogenic foreland sedimentary rocks. This indicates that foreland basin sediments were partly tectonically interleaved with the pre-orogenic metasediments of the Brusque Complex during late-stage orogenic deformation. The findings support an intracontinental rifting model for the formation of the Kaoko–Dom Feliciano–Gariep basin system. The data further indicate that the Luis Alves Craton was in close proximity to the Congo Craton, and likely with the Nico Pérez Terrane and the Kalahari Craton, at the onset of Tonian rifting and the breakup of Rodinia.

1. Introduction

The period between the breakup of Rodinia and the amalgamation of Gondwana during the Neoproterozoic (ca. 800 to 500 Ma) is interpreted to involve the reconfiguration of many of Earth's major cratonic blocks (Johansson, 2014; Li et al., 2008; Merdith et al., 2017a, 2017b). Paleogeographic reconstructions at the time of Rodinia breakup vary significantly in the placement of continental blocks that now belong to the African and South American continents. Some models place the African and South American cratons as close neighbours (Johansson, 2014; Li et al., 2008, 2013), and in other models they are far apart with a large oceanic domain between them (Evans, 2009; Gray et al., 2008; Merdith et al., 2017a). The latter models contrast with tectonic reconstructions of the orogenic belts exposed today along the South Atlantic coastlines, in which authors assume that there was no major reconfiguration of continental blocks and instead suggest that pairs of previously rifted continental margins came back together during their convergent evolution (Basei et al., 2018; Frimmel et al., 2011;

* Corresponding author at: Department of Geosciences, UiT – The Arctic University of Norway, Dramsveien 201, 9037 Tromsø, Norway.
E-mail address: jack.j.percival@uit.no (J.J. Percival).

https://doi.org/10.1016/j.precamres.2020.106060
Received 18 August 2020; Received in revised form 7 December 2020; Accepted 7 December 2020
Available online 30 December 2020

Konopásek et al., 2018, 2020; Oriolo et al., 2016; Porada, 1989).

The breakup of Rodinia and the transition into what would become Western Gondwana began with extensive early-Neoproterozoic rifting at ca. 840–800 Ma (Basei et al., 2008b; Frimmel et al., 2001, 2011; Hueck et al., 2018a; Konopásek et al., 2014, 2018; Porada, 1989), which developed by way of convergence into orogenesis active between ca. 650–550 Ma (Hueck et al., 2018b; Konopásek et al., 2008; Lenz et al., 2011; Oyhantçabal et al., 2009), leaving behind a ca. 3000 km long orogen recently named the South Atlantic Neoproterozoic Orogenic System (SANOS) (Konopásek et al., 2020). The southern part of this system (Fig. 1) is an orogenic triple junction comprised of multiple orogenic belts: the Kaoko, Dom Feliciano and Gariep belts forming a North–South oriented belt continuous with the rest of the SANOS, and the Damara Belt forming an offshoot junction on the African side of the orogen. In the Kaoko–Dom Feliciano–Gariep part of this system, orogenesis was the result of convergence between the Congo and Kalahari cratons on the African side, and the Rio de la Plata craton and other smaller crustal blocks such as the Luis Alves Craton and Nico Pérez and Curitiba terranes on the South American side (Basei et al., 2000, 2009; Frimmel et al., 2011; Frimmel, 2018; Goscombe et al., 2003b; Hueck et al., 2018b; Oriolo et al., 2016). The pre-convergent evolution of this orogenic system is an extensively discussed topic, as it provides context in linking through time the breakup of Rodinia and the amalgamation of Western Gondwana. Central to these discussions is whether early-Neoproterozoic rifting culminated in breakup of the crust and the development of a large ocean known as the Adamastor Ocean (see Fig. 2 in Konopásek et al., 2020; and references therein), and thus the exact pre-orogenic connections between the African and South American parts of the Kaoko–Dom Feliciano–Gariep orogen remains an important line of research (e.g. Basei et al., 2005, 2011c; Oyhantçabal et al., 2018). Recent works have correlated the convergent history of rocks of the orogenic hinterland across both the Kaoko and Dom Feliciano Belts (Gross et al., 2009; Konopásek et al., 2016; Oyhantçabal et al., 2009, 2011a); however, connecting the pre-convergence histories of the two belts so far remains problematic.

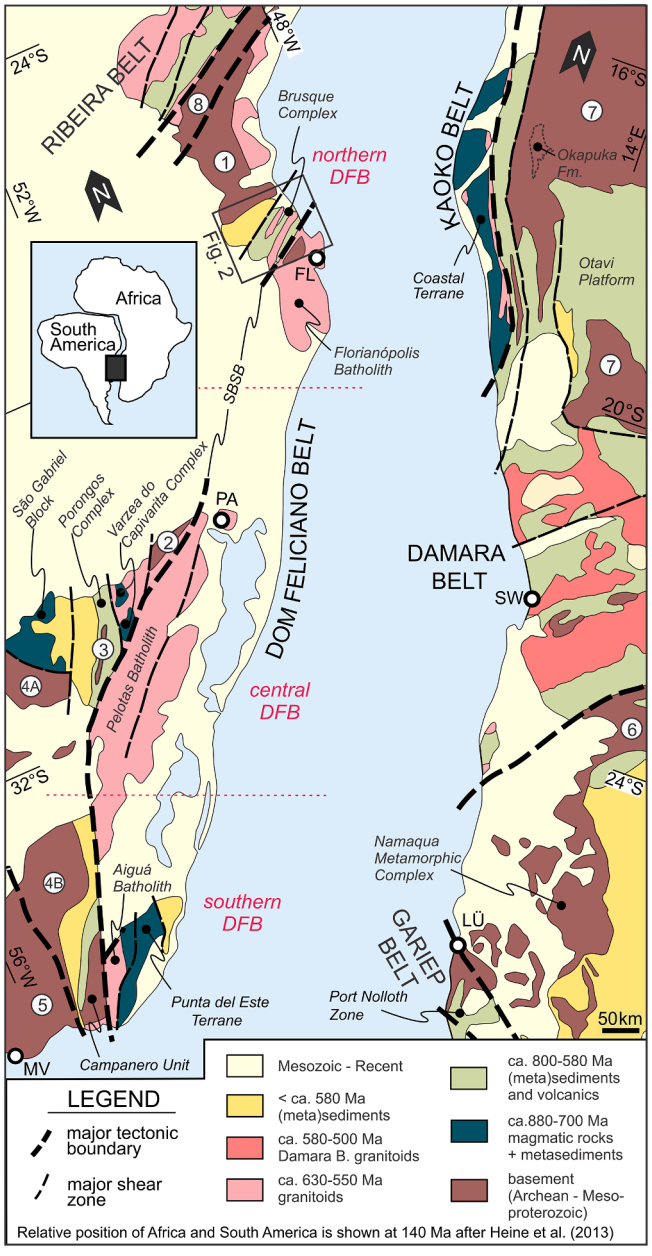

Fig. 1. Overview geological sketch of the Kaoko–Dom Feliciano–Gariep orogenic system (modified after Konopásek et al., 2017). 1—Luis Alves Craton, 2—Arroio dos Ratos Complex, 3—Encantadas Complex, 4A—Nico Pérez Terrane (Taquarembó Block), 4B—Nico Pérez Terrane, 5—Rio de la Plata Craton, 6—Kalahari Craton, 7—Congo Craton, 8—Curitiba Terrane. SBSB—Southern Brazilian Shear Belt, FL—Florianópolis, PA—Porto Alegre, MV—Montevideo, LÜ—Lüderitz, SW—Swakopmund.

Some of the most promising targets for investigation of the early history of the orogen are the supracrustal schist belts that run the length of the orogen, and that outcrop on both sides of the Atlantic Ocean. These units are interpreted as rifting-related basin deposits (Basei et al., 2008b; Campos et al., 2011; Frimmel and Fölling, 2004; Frimmel, 2018; Konopásek et al., 2014; Saalmann et al., 2006) that were later deformed and metamorphosed in the foreland positions of the orogen (Basei et al., 2011b; Frimmel et al., 2011; Frimmel, 2018; Goscombe et al., 2003b; Saalmann et al., 2006). As such, they should contain a record of the pre-convergence history from rifting to the onset of orogenesis.

The aim of this work is to discuss the mutual pre-orogenic positions of rifted margins of the Congo and Luis Alves cratons by studying the depositional history and potential source regions of the supracrustal rocks of the northern Dom Feliciano Belt using U–Pb detrital zircon geochronology. If the African and South American cratons represented one coherent crustal block at the beginning of rifting, the provenance record of metamorphosed rifting-related sediments on top of them should correlate. Studies with large datasets have been published investigating the timing of sedimentation and potential sources for these supracrustal rocks in the African counterpart of the belt (the Kaoko and Gariep orogenic belts) (Andersen et al., 2018a; Hofmann et al., 2014; Konopásek et al., 2014, 2017). Similarly, the central parts of the Dom Feliciano Belt are well studied (Gruber et al., 2011, 2016; Höfig et al., 2018; Pertille et al., 2015a, 2015b, 2017) (for a current review of the relevant provenance record in Western Gondwana, see Zimmermann, 2018). However, there is little data for the northern part of the belt (Basei et al., 2008a; Hartmann et al., 2003), which represents the direct counterpart to the Kaoko Belt in a pre-Atlantic setting (Fig. 1). We present a robust dataset of detrital zircon ages from metamorphosed clastic sedimentary and igneous rocks of the northern Dom Feliciano foreland that enables comparison and possible correlation of syn-rifting evolution with the Kaoko Belt in Africa, as well as with the central and southern Dom Feliciano Belt.

2. Geological setting

2.1. The Kaoko–Dom Feliciano–Gariep orogenic system

The Kaoko, Dom Feliciano and Gariep belts (Fig. 1) are three geographically separate orogenic belts that, prior to the opening of the Atlantic Ocean, represented a continuous orogenic system formed during the Neoproterozoic Brasiliano/Pan African orogenic cycle (Porada, 1989). The system crops out along the South Atlantic coastlines of South

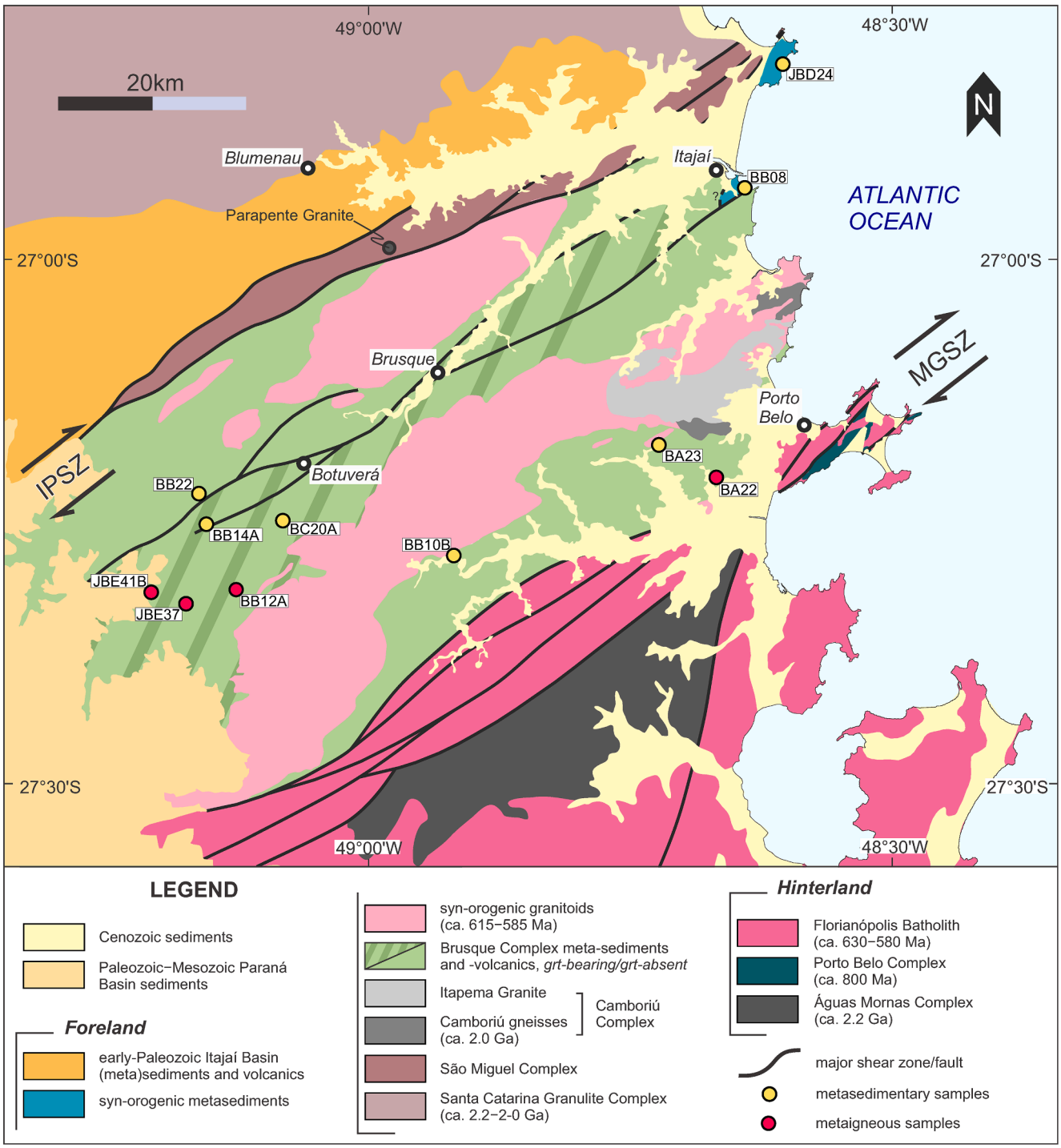

Fig. 2. Geological map of the northern Dom Feliciano Belt foreland. MGSZ = Major Gercino Shear Zone, IPSZ = Itajaí–Perimbó Shear Zone. Modified after Basei et al. (2006); Campos et al. (2011); De Toni et al. (2020a); Florisbal et al. (2012b); Hueck et al. (2018b). See text for geochronological references.

America and Africa, and forms the southern part of the larger South Atlantic Neoproterozoic Orogenic System (*sensu* Konopásek et al., 2020). The Kaoko–Dom Feliciano–Gariep orogenic system is structurally symmetric, with an eastern and western foreland domain lying either side of an internal orogenic hinterland (Fig. 1). Both foreland domains contain fold-and-thrust belts incorporating early- to middle-Neoproterozoic rift-related volcano-sedimentary rocks and associated basement, overlain by syn-orogenic flysch and molasse deposits (Frimmel, 2018; Goscombe et al., 2003b; Hueck et al., 2018b).

The basement of the eastern foreland consists of the Archean–Paleoproterozoic Congo and Kalahari cratons, and associated Mesoproterozoic crust exposed along the cratons' western edges (Kröner and Rojas-Agramonte, 2017; Kröner et al., 2004; Macey et al., 2018; Seth et al., 1998) (Fig. 1). In the Kaoko Belt, the eastern-most part of the foreland consists of autochthonous early- to middle-Neoproterozoic sedimentary successions lying directly on the Congo Craton basement, named the Otavi Carbonate Platform (Hoffman and Halverson, 2008). The low-grade Otavi Carbonate Platform is overridden by an imbricated fold-and-thrust belt, the Central Kaoko Zone, which consists of deformed and metamorphosed early- to middle-Neoproterozoic sedimentary

successions interlayered with slices of the basement, and overlain by late-Neoproterozoic syn-orogenic sedimentary rocks (Konopásek et al., 2014, 2017). The equivalent unit in the Gariep Belt is the para-utochthonous Port Nolloth Zone, which comprises all Neoproterozoic sedimentary rocks within the fold-and-thrust belt including rift-related basin deposits overlain by foredeep sediments (Frimmel et al., 1996; Frimmel, 2018 and references therein). The Port Nolloth Zone is overridden by the allochthonous Marmora Terrane, consisting of post-rift oceanic metabasalts overlain by late-Neoproterozoic siliciclastic and carbonate sedimentary rocks (Frimmel and Fölling, 2004; Frimmel, 2018).

The orogenic hinterland outcrops on both sides of the Atlantic Ocean, and consists of tectonically interleaved orthogneisses, paragneisses and migmatites intruded by numerous late-Neoproterozoic plutons. It is represented by the Coastal Terrane in the Kaoko Belt (Goscombe et al., 2005b), and the Cerro Olivo Complex of the Punta del Este Terrane, the Várzea do Capivarita Complex, and the Porto Belo and Águas Mornas Complexes in the southern, central and northern Dom Feliciano Belt respectively (Fig. 1) (Battisti et al., 2018; De Toni et al., 2020a; Gross et al., 2009; Oyhantçabal et al., 2009; Silva et al., 2000). The protoliths of the metamorphic hinterland consist of Paleoproterozoic cratonic basement intruded by early-Neoproterozoic bimodal magmatic rocks that are interpreted as remnants of arc-related (De Toni et al., 2020a; Koester et al., 2016; Lenz et al., 2013; Martil et al., 2017; Philipp et al., 2016) or rift-related (Konopásek et al., 2018; Oyhantçabal et al., 2009; Will et al., 2019) magmatism, and associated sedimentary cover. The episodic crustal stretching, melting and basin sedimentation that formed the early-Neoproterozoic parts of the hinterland rocks occurred from ca. 840 Ma to at least ca. 710 Ma (Basei et al., 2011c; De Toni et al., 2020a; Konopásek et al., 2014; Lenz et al., 2011; Martil et al., 2017; Oyhantçabal et al., 2009), and likely up to ca. 660–650 Ma ending shortly before the onset of orogenesis (Konopásek et al., 2017, 2018; Kröner et al., 2004). Orogenesis coincides with a strong metamorphic overprint in the hinterland rocks at ca. 670–640 Ma (Chemale et al., 2012; Masquelin et al., 2012; Oyhantçabal et al., 2009).

Along the western edge of the hinterland, in the Dom Feliciano Belt, is the Granite Belt: an extensive belt of late-Neoproterozoic, syn- and post-collisional granitoid batholiths (Fig. 1) (Bitencourt and Nardi, 1993, 2000; Florisbal et al., 2009, 2012a, 2012b; Hueck et al., 2018b; Oyhantçabal et al., 2007; Philipp and Machado, 2005; Philipp et al., 2013), that intrude the Paleoproterozoic to early-Neoproterozoic units of the high-grade hinterland (De Toni et al., 2020a; Koester et al., 2016; Lenz et al., 2013; Martil et al., 2017; Masquelin et al., 2012). The granitoids predominantly intruded between ca. 630–580 Ma (Florisbal et al., 2012b; Lara et al., 2020; Philipp and Machado, 2005), with scattered evidence of early magmatism at ca. 660–650 Ma (Chemale et al., 2012; Frantz et al., 2003).

The Granite Belt is in tectonic contact with the western foreland, separated by a large strike-slip dominated shear zone system running the entire length of the Dom Feliciano Belt, known as the Southern Brazilian Shear Belt (Fig. 1) (Bitencourt and Nardi, 2000). The foreland consists of a fold-and-thrust belt comprised of pre-orogenic rift-related sedimentary successions – known as the Schist Belt – and their associated basement rocks (Basei et al., 2011b; Bettucci et al., 2001; Saalmann et al., 2006), and a system of foreland basins (Fig. 1) (Almeida et al., 2010; Basei et al., 2011a; Guadagnin et al., 2010; Hueck et al., 2018b). The Schist Belt is comprised of the Brusque, Porongos and Lavalleja complexes in the Northern, Central and Southern Dom Feliciano Belt respectively. The Schist Belt and foreland basins lie on Archean–Paleoproterozoic basement units (Fig. 1). In Uruguay, the basement of the Dom Feliciano Belt foreland is the Nico Pérez Terrane (Oriolo et al., 2016; Oyhantçabal et al., 2011b). In the Central Dom Feliciano Belt, the basement of the foreland is exposed as tectonic windows in the Schist Belt (Saalmann et al., 2006).

2.2. The northern Dom Feliciano Belt

The foreland basement of the northern Dom Feliciano Belt is the Luis Alves Craton, which is predominantly comprised of Paleoproterozoic granulitic gneisses of the Santa Catarina Granulite Complex (Fig. 2) (Basei et al., 2009; Hartmann et al., 2015; Passarelli et al., 2018). The complex is made up of ca. 2.2–2.0 Ga orthogneisses, interspersed with mafic–ultramafic enclaves and subordinate paragneisses (Basei et al., 1998a, 2009; Hartmann et al., 1999, 2000). The southern margin of the Luis Alves Craton is covered by the Itajaí Basin (Fig. 2) (Basei et al., 2009; Passarelli et al., 2018), which consists of volcano-sedimentary successions deposited in an orogenic foreland environment (Basei et al., 2011a) with a maximum age of deposition constrained by U–Pb zircon dating of interlayered volcanics at ca. 560–550 Ma (Guadagnin et al., 2010). The Itajaí Basin is weakly deformed, with deformation increasing south-eastwards towards the Itajaí–Perimbó Shear Zone where it is in contact with the foreland fold-and-thrust belt (Fig. 2) (Basei et al., 2011a).

The fold-and-thrust belt is predominantly comprised of metamorphosed volcano-sedimentary sequences of the Brusque Complex intruded by a series of Neoproterozoic granitoids between ca. 630–585 Ma (Fig. 2) (Florisbal et al., 2012b; Hueck et al., 2019). A narrow sliver of crystalline basement of unknown age and origin, known as the São Miguel Complex, is exposed at the north-western contact with the Itajaí Basin (Fig. 2) (Basei et al., 2011b). Syenogranites intruding this foreland basement have been dated at 835 ± 9 Ma and 843 ± 12 Ma (U–Pb zircon), and are interpreted as A-type granitoids marking the beginning of rifting that lead to the formation of the Brusque Complex paleobasin (Parapente Granite, see Fig. 2) (Basei et al., 2008b). This is within error of a 833 ± 3 Ma (U–Pb zircon) age found in granitic to syenitic rocks of the Richtersveld Igneous Complex in the Gariep Belt, which is similarly interpreted as evidence of the earliest crustal thinning in the region marking the beginning of continental breakup (Frimmel et al., 2001).

A basement inlier—the Camboriú Complex—outcrops along the coast in central part of the Brusque Complex (Fig. 2). The Camboriú Complex is predominantly comprised of migmatitic felsic orthogneisses interleaved with amphibolites (Martini et al., 2019), which predominantly show U–Pb zircon ages of 2.2–2.0 Ga comparable with the Luis Alves Craton (Hartmann et al., 2003; Silva et al., 2000, 2005).

The southern border of the Brusque Complex is in tectonic contact with the Florianópolis Batholith, and the two units are separated by the large-scale Major Gercino Shear Zone (Fig. 2). The Florianópolis Batholith is the northern exposure of the Granite Belt (Fig. 1), and is comprised of a vast series of Neoproterozoic granitoids that intruded the western edge of the hinterland represented by the ca. 800 Ma migmatitic orthogneisses of the Porto Belo Complex (De Toni et al., 2020a) and the Paleoproterozoic Águas Mornas Complex (Fig. 2) (Silva et al., 2005). The granitoids were emplaced predominantly between ca. 630–590 Ma (Chemale et al., 2012; Florisbal et al., 2012b).

2.3. Early evolution of the Brusque Complex

The rocks in this study belong to the metamorphosed volcano-sedimentary successions of the Brusque Complex, which forms a NE–SW oriented belt of predominantly pelitic schists divided into a northern and southern section by an elongate syn-orogenic granitic batholith (Fig. 2) (Valsungana Batholith). Metamorphism in the Brusque Complex is characterised by a general increase in metamorphic grade from NW–SE (Basei et al., 2011b; Campos et al., 2011, 2012). In the NW, the Brusque Complex metapelites are dominated by lower-greenschist facies chlorite – mica schists and phyllites, and a narrow garnet zone in the centre and southern parts of the belt suggests metamorphic conditions reached maximum lowermost amphibolite facies (Fig. 2). The Brusque Complex rocks are intensely deformed, showing evidence of multiple deformation structures associated with its prolonged contractional history (Basei et al., 2011b; Campos et al., 2011).

There is little published work available concerning the early evolution of the Brusque Complex, as poor exposure and the intensity of deformation makes any stratigraphic subdivision difficult. Despite this, three sequences are generally described based on the presence or absence of volcanic sub-units (e.g. Basei et al., 2006, 2011b). The lowermost and upper-most formations—the Rio do Oliveira and Rio da Areia sequences respectively—are described as being dominated by metasedimentary rocks, with some mafic and rare felsic metavolcanics interlayered within (Basei et al., 2011b; Campos et al., 2011). The upper sequence is described as containing a large proportion of metacarbonate rocks, and the lower sequence frequently containing calc-silicate lenses of volcanogenic origin (Basei et al., 2011b; Campos et al., 2011). The middle formation—the Botuverá sequence—is described as entirely clastic, varying in composition between metapelitic and metapsammitic and containing no metavolcanic or metacarbonate rocks (Basei et al., 2011b).

There is also little published data to constrain the timing of sedimentation of the Brusque Complex protolith. The upper limit is loosely placed at ca. 840 Ma at the start of basin formation (Basei et al., 2008b), but within the Brusque Complex itself there are currently no reliable constraints on the upper limit of sedimentation. Basei et al. (2008a) reported a minimum age at ca. 570–540 Ma based on the two youngest detrital zircon grains from pelitic schists of the Brusque Complex. However, this age is contradicted by the well-constrained age of intrusion of granitic plutons and dykes into the Brusque Complex metasediments between ca. 620 and 580 Ma (Campos et al., 2012; Hueck et al., 2019). Currently, these post-metamorphic magmatic rocks remain the only robust constraint on the minimum age of sedimentation into the Brusque Complex paleobasin.

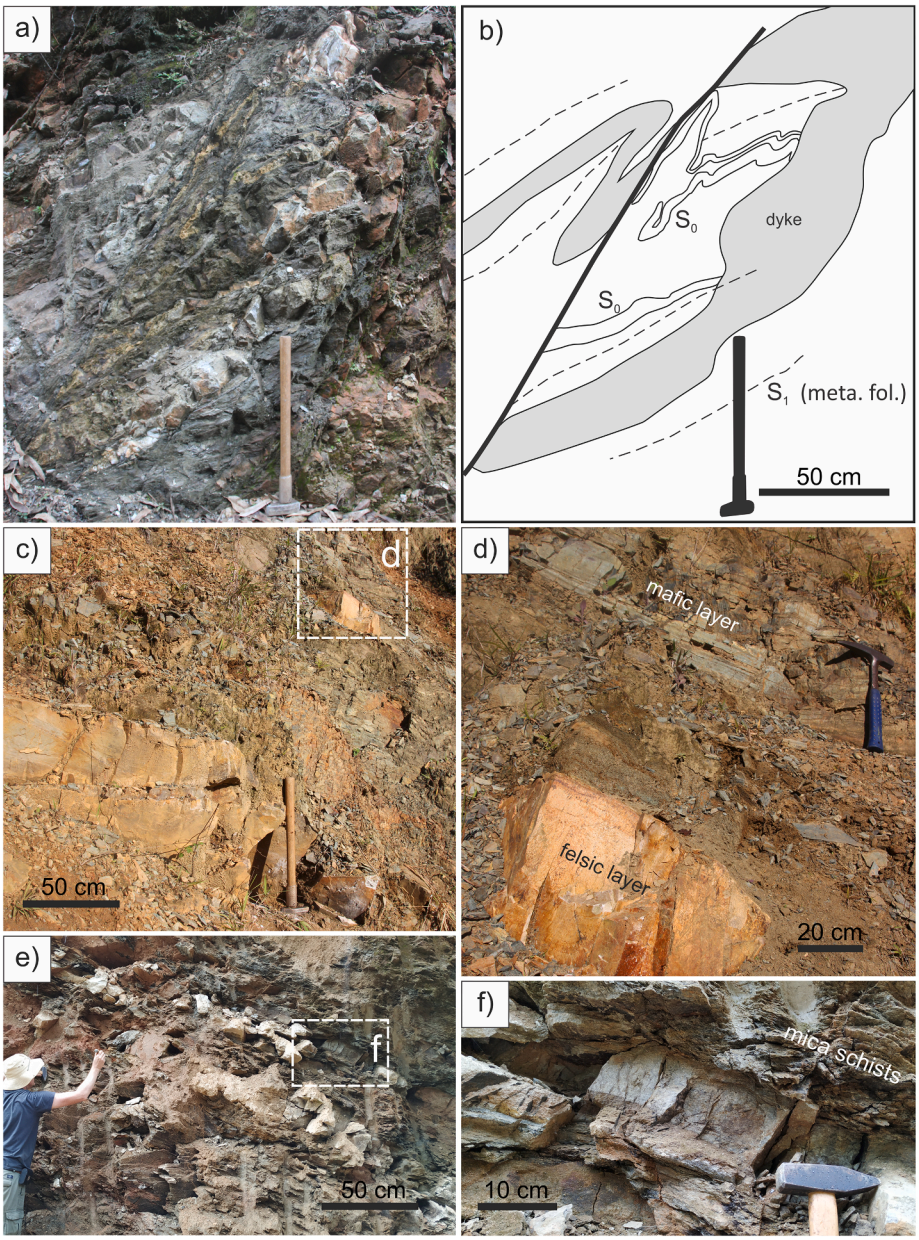

Fig. 3. Outcrops of metaigneous rocks: a) photo of the metamorphosed and deformed felsic dyke BB12A, b) an accompanying sketch of the same road-cut outcrop outlining the cross-cutting nature of the dyke relative to remnant S_0, c) road-cut outcrop BA22, d) detail of outcrop BA22 showing bimodal volcanics, e) outcrop JBE37, f) detail of outcrop JBE37 showing foliation-parallel nature of felsic rock.

3. Geochronology

3.1. Materials and methods

Zircon U–Pb ages were determined at the Institute of Geology of the Czech Academy of Sciences, Prague, Czech Republic, using laser ablation inductively coupled plasma mass spectrometry (LA-ICP-MS), and the complete isotopic dataset is presented in Electronic Appendix A. For detrital zircon data, U–Pb age spectra are presented as cumulative distribution curves with 95% confidence intervals after Andersen et al. (2016) and using the visualisation package (*detzrcr*) of Andersen et al. (2018b), and as frequency histograms with 30 Ma binwidths and adaptive kernel density estimate (KDE) curves as described in Vermeesch et al. (2016) using the software package (*densityplotter* version 8.4) of Vermeesch (2012). Only concordant dates with calculated discordance within ± 10%, are included. Concordance is calculated from ages, using ($^{206}Pb/^{238}U$) / ($^{207}Pb/^{206}Pb$) for $^{207}Pb/^{206}Pb$, and using ($^{206}Pb/^{238}U$) / ($^{207}Pb/^{235}U$) for $^{206}Pb/^{238}U$. $^{207}Pb/^{206}Pb$ dates are reported for data > 1.0 Ga, and $^{206}Pb/^{238}U$ dates for data < 1.0 Ga. Description of zircon separation and analytical methods is provided in Electronic Appendix B. Locations of analysed samples are plotted in Fig. 2.

3.2. Description of metaigneous samples and results of U–Pb zircon dating

3.2.1. Sample BB12A

Sample BB12A (Fig. 2) (27° 18.940′ S, 49° 07.682′ W) was collected from a felsic dyke intrusive in metapelitic schists. The dyke is approximately 30 cm thick, and is folded and metamorphosed together with the schists indicating intrusion prior to deformation and metamorphism of the host rock (Fig. 3a and b). The metamorphic mineral assemblage is dominated by quartz, plagioclase and K-feldspar, with minor white mica, chlorite and biotite, and accessory opaque minerals. Chlorite pseudomorphs after garnet completely replace poikiloblastic garnet, suggesting overprint at lower metamorphic conditions. The original magmatic texture has been almost completely overprinted by metamorphism and deformation, although K-feldspar crystals much larger than those in the matrix remain as inclusions in garnet pseudomorphs suggesting that the magmatic fabric is locally preserved.

From 42 spot analyses in oscillatory-zoned parts of the zircon grains, 25 concordant dates combine in a concordia U–Pb age of 811 ± 6 Ma (Fig. 4a and b), interpreted as the age of intrusion and crystallisation of the dyke. Zircon grains range from ca. 60 to 150 μm in length, and most are idiomorphic and show oscillatory zoning in cathodoluminescence (CL) images (Fig. 4c). Some grains show truncated zoning at the edges, which are likely fractured and abraded inherited zircons. Of the remaining 17 analyses, three are discordant likely due to lead loss at an unspecified time, and the rest are older than the major cluster of dates and likely represent inherited grains.

3.2.2. Sample BA22

Sample BA22 (27° 12.195′ S, 48° 39.853′ W) is a fine-grained metarhyolite, consisting of quartz, plagioclase, K-feldspar, minor amounts of muscovite, and with accessory garnet and opaque minerals. The outcrop consists of a series of metamorphosed, interlayered mafic and felsic volcanic rocks interspersed with metapelitic schists (Fig. 3c and d). The outcrop shows a penetrative metamorphic foliation, overprinting any previous magmatic texture. However, due to layering of the mafic, felsic and pelitic layers, and the presence of abundant K-feldspar, we interpret the sample as a metamorphosed felsic volcanic rock.

Only a small number of zircon grains were recovered from the sample, varying between 70 and 190 μm in length and 60 and 130 μm in width. The grains predominantly show sector zoning, with minor oscillatory zoning, and are strongly fractured and rounded. Of 22 grains analysed, 19 yielded concordant dates. Four grains were analysed twice, and repeated dates were not plotted. The data are plotted in Fig. 5a, and show that the dates mainly cluster at ca. 2.05 Ga. Due to similarities with the surrounding samples (see below), we interpret all zircon grains as inherited.

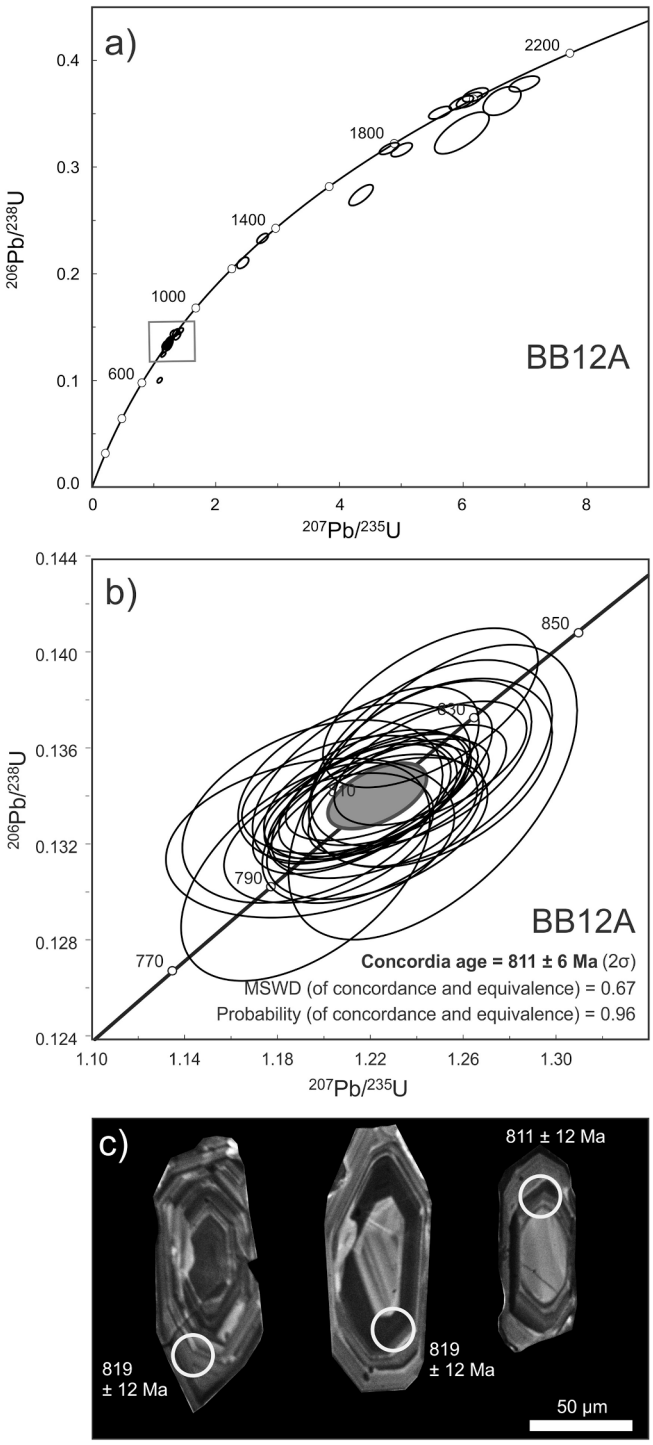

Fig. 4. Results of U–Pb zircon dating of sample BB12A: a) zircon U–Pb concordia plot for sample BB12A (analysed by LA–ICP–MS), b) detail of inset showing combined 25 data points used for calculation of the concordia age (data point error ellipses are plotted at 2σ level, MSWD = mean square weighted deviation), and c) cathodoluminescence images and individual dates of example zircon grains.

3.2.3. Sample JBE41B and JBE37

Samples JBE41B (27° 19.083′ S, 49° 12.516′ W) and JBE37 (27°

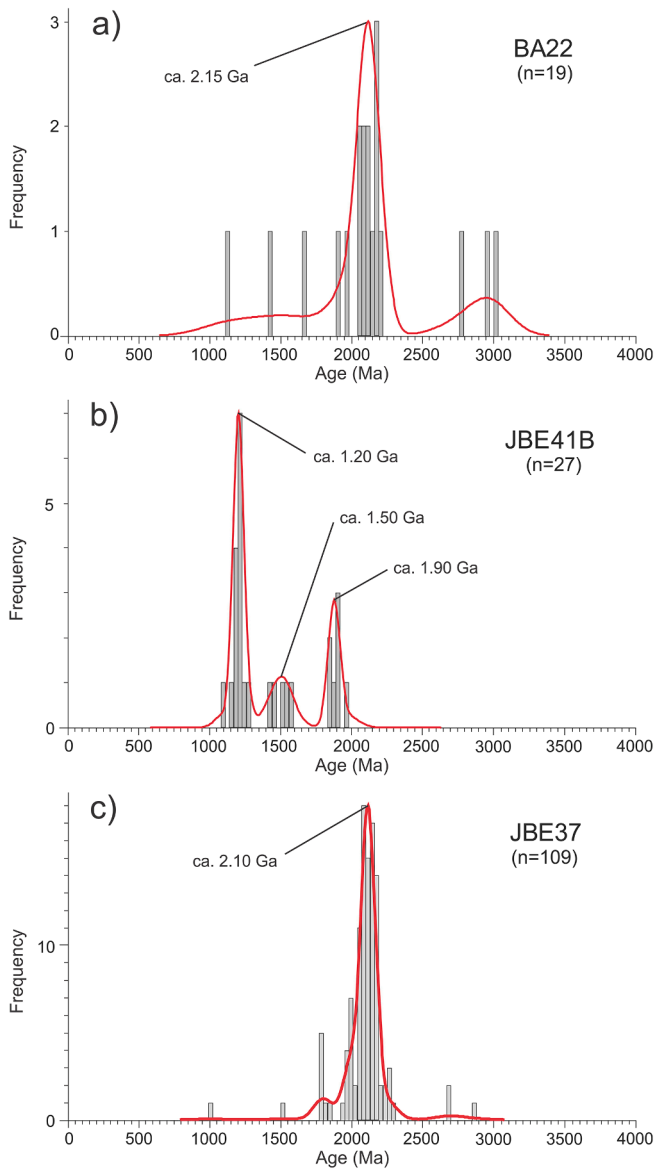

Fig. 5. U-Pb zircon age data for analysed metaigneous samples, presented as frequency histograms and KDEs. n = number of data.

20.192′ S, 49° 10.536′ W) were collected from approximately foliation-parallel felsic layers within the garnet-schists of the Brusque Complex. Both outcrops consist of a series of felsic layers approximately 10–30 cm thick, interlayered with garnet-bearing schists. The samples contain the mineral assemblage quartz, plagioclase and K-feldspar, with subordinate biotite, white mica, chlorite and opaque minerals. Chlorite pseudomorphs after garnet in sample JBE37 contain K-feldspar inclusions similar to sample BB12A. Based on field observations and the presence of blastoporphyritic K-feldspar, we interpret the protoliths of the samples as metamorphosed felsic volcanic rocks. However, due to metamorphic overprint it remains difficult to conclusively differentiate them from a meta-arkose.

For sample JBE41B, 28 zircon grains were analysed and 27 yielded concordant dates with 2σ uncertainty ≤ 10%. The data are plotted in Fig. 5b, and the resulting spectrum shows age peaks at ca. 1.90, 1.50 and 1.20 Ga. All of the zircon grains are interpreted as inherited/detrital.

For sample JBE37, analysis of 112 zircon grains produced 109 concordant dates with 2σ uncertainty ≤ 10%. The data are plotted in Fig. 5c, and the resulting spectrum shows a single dominant age peak centred at ca. 2.10 Ga, with a much smaller peak at ca. 1.80 Ga, and some individual data between ca. 3.00–1.00 Ga. All of the zircon grains are also interpreted as inherited/detrital.

3.3. Description of metasedimentary samples and results of U–Pb detrital zircon dating

3.3.1. Sample JBD24

Sample JBD24 (26° 48.324′ S, 48° 35.838′ W) is a micaceous quartzite collected from within the Itajaí–Perimbó Shear Zone, close to the northern contact with the underlying basement (Basei et al., 2011b) (Fig. 2). The rock is intensely folded and deformed, though weakly metamorphosed, containing quartz, muscovite, biotite, chlorite and plagioclase, with accessory opaque minerals. Zircon grains are mostly ca. 50 to 120 μm in length, and show varying degrees of fragmentation from whole, prismatic crystals to small, abraded fragments. The majority show oscillatory zoning, and often with truncated edges likely due to transport and abrasion. No grains appear to have metamorphic overgrowth rims, and few show sector zoning or no zoning at all.

Analysis of 140 grains yielded 118 concordant dates. The spectrum of dates (Fig. 6a) shows distinct peaks at ca. 2.20 Ga and 660 Ma, with individual data in the intervals between ca. 2.10–0.80 Ga, and ca. 3.60–2.30 Ga.

3.3.2. Sample BB08

Sample BB08 (26° 55.544′ S, 48° 38.055′ W) is a carbonate-bearing phyllitic metarhythmite collected from a coastal outcrop within the southern part of the Itajaí–Perimbó Shear Zone (Fig. 2). The rock is strongly deformed, with a primary metamorphic foliation containing intrafolial folding that is overprinted by a steep, pervasive crenulation cleavage parallel to the Itajaí–Perimbó Shear Zone. The style of deformation at this outcrop is consistent with other high-strain parts of the Brusque Complex (Basei et al., 2011b).

The rock contains quartz, muscovite, biotite, chlorite, plagioclase and calcite, with accessory opaque minerals. Zircon grains vary between ca. 60 and 200 μm in length. Most of the grains show oscillatory zoning, with some showing sector zoning and other more complex internal structures. The majority of grains are abraded and fragmented, and some show thin CL-bright overgrowth rims.

101 analysed zircon grains yielded 82 concordant dates. The data show a similar bimodal distribution to sample JBD24, with distinct peaks at ca. 2.15 Ga and 670 Ma, and minor peaks at ca. 625 and 560 Ma (Fig. 6b). Individual data appear over the intervals between ca. 2.95–1.75 Ga and ca. 750–500 Ma. The two youngest individual zircon grains are ca. 84 Ma and 375 Ma, which are significant outliers. These two grains are likely from contamination, either from beach sediment cemented onto the rock by dissolution and precipitation of calcite, or otherwise introduced during the separation process.

3.3.3. Sample BA23

Sample BA23 (27° 10.511′ S, 48° 43.054′ W) was collected in the southeast section of the Brusque Complex from a large, loose block at the foot of an isolated steep slope (not in situ, but inferred to be close to its original position on the hill above). The sample is a weakly foliated micaceous quartzite containing quartz, muscovite, biotite, chlorite and garnet, with accessory opaque minerals. Zircon grains range between ca. 80 and 150 μm in length, and are mostly fragmented and abraded. Most grains have oscillatory or sector zoning, and many show featureless overgrowth rims. A smaller number show complex zoning patterns or no zoning at all.

Isotopic dating yielded 136 concordant dates from 140 analysed zircon grains. The age spectrum (Fig. 6c) shows the majority of dates cluster at a single peak ca. 2.00 Ga. A minor, long-wavelength peak centred at 2.70 Ga encompasses a series of individual dates between ca. 3.15–2.30 Ga.

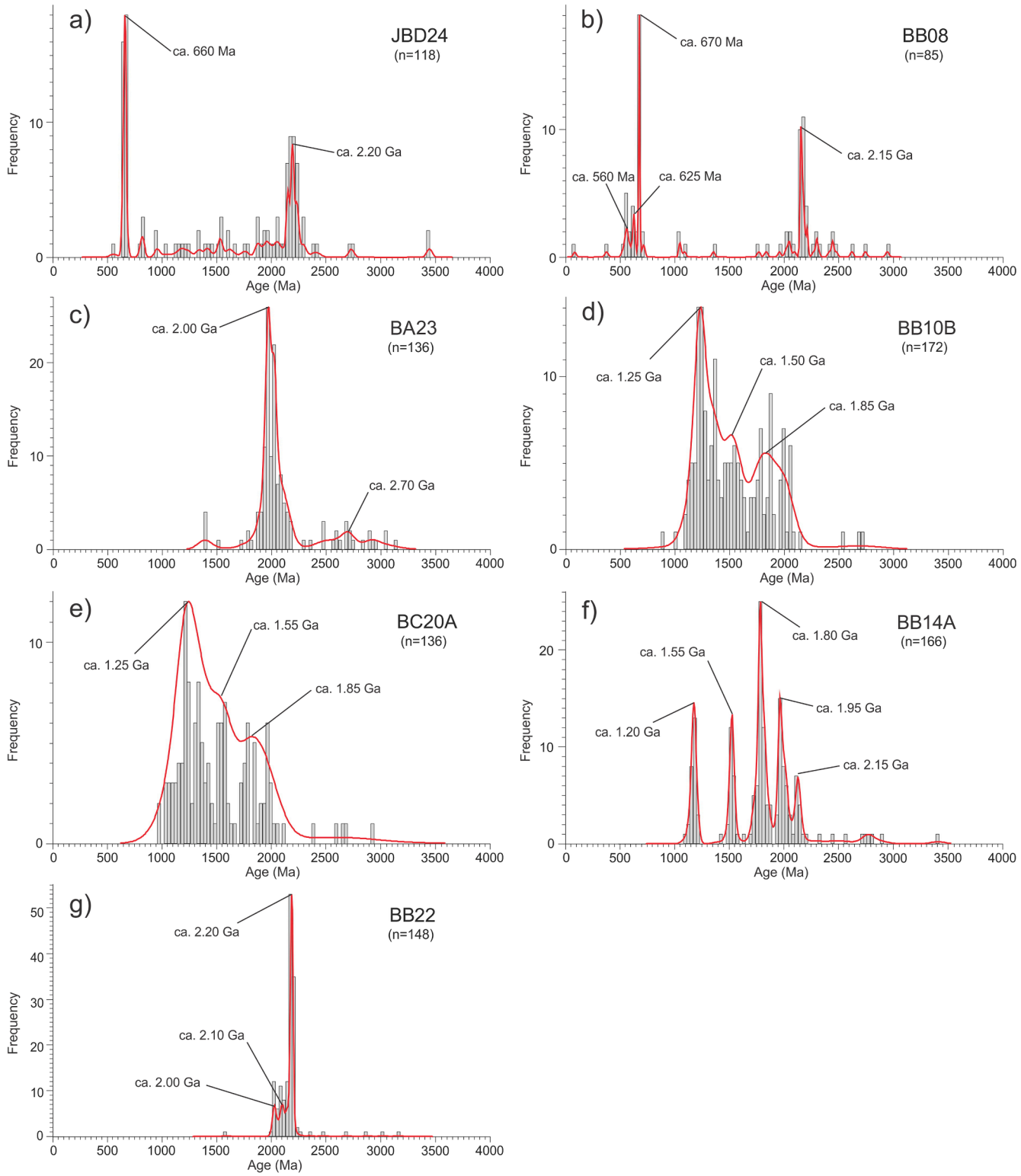

Fig. 6. U-Pb detrital zircon data for analysed metasedimentary samples, presented as frequency histograms and KDEs. n = number of data.

3.3.4. Sample BB10B

Sample BB10B (27° 16.964′ S, 48° 55.006′ W) was collected from the southern-central part of the Brusque Complex, from a strongly foliated quartz-rich schist containing quartz, muscovite, biotite, and chlorite, with accessory opaque minerals. Zircon grains range from ca. 50 to 120 μm in length, and ca. 30 to 50 μm in width. Many grains are elongate and euhedral, showing sector or oscillatory zoning. Thin, CL-bright overgrowth rims are common.

Analysis of 182 zircon grains yielded 172 concordant dates. The spectrum of ages (Fig. 6d) shows a broad distribution of dates from ca. 2.20–1.00 Ga, with the highest proportion centred at a peak at ca. 1.25 Ga. The remaining data are distributed between ca. 2.20–1.30 Ga with minor peaks at ca. 2.00, 1.80, 1.50 and 1.35 Ga.

3.3.5. Sample BC20A

Sample BC20A (27° 14.919′ S, 49° 04.959′ W) was collected from a strongly deformed garnet-bearing schist in the south-western part of the Brusque Complex. The sample contains quartz, garnet, muscovite, biotite, chlorite and plagioclase, with accessory tourmaline and opaque minerals. Zircon grains range from ca. 50 to 200 μm in length. Grains vary in shape and structure: some are euhedral with oscillatory zoning, while others have abraded edges, are often fractured, and with complex internal structures.

Isotopic analysis of 140 zircon grains produced 136 concordant dates. The data (Fig. 6e) show a broad distribution of dates between ca. 2.10 Ga and 900 Ma, with a major peak at ca. 1.25 Ga and minor peaks at ca. 1.95, 1.80, 1.55 and 1.35 Ga.

3.3.6. Sample BB14A

Sample BB14A (27° 15.128′ S, 49° 09.412′ W) is a quartzite collected from the western part of the Brusque Complex. The sample contains quartz, muscovite and biotite, with accessory rutile and opaque minerals. Zircon grains range from ca. 80 to 200 μm in length, and are predominantly elongate and rounded. Most grains show oscillatory zoning, with only a few showing sector or complex zoning patterns. The grains are mostly fragmented and abraded

From 168 zircon grains analysed, 166 produced concordant U–Pb dates. The resulting age spectrum (Fig. 6f) shows distinct peaks at ca. 2.15, 1.95, 1.80, 1.55 and 1.15 Ga.

3.3.7. Sample BB22

Sample BB22 (27° 13.358′ S, 49° 09.847′ W) is a quartzite collected from the low-grade section of the Brusque Complex in the north-west. The sample contains quartz and muscovite, with accessory titanite and opaque minerals. Zircon grains range from 70 to 250 μm in length, and are predominantly elongate and rounded. Most grains show oscillatory zoning, and are mostly fragmented and abraded. Some grains show more complex zoning patterns.

Isotopic analysis of 154 zircon grains produced 148 concordant U–Pb dates. The corresponding age spectrum (Fig. 6g) shows the majority of dates centred at a large peak at ca. 2.20 Ga, with two minor peaks at ca. 2.10 and 2.05 Ga.

4. Discussion

4.1. Constraining the age of sedimentation

The concordia U–Pb zircon age of 811 ± 6 Ma from sample BB12A represents the youngest cluster of data in the sample, and likely the crystallisation age of the dyke. Because the youngest detrital zircon grains from neighbouring samples (e.g. BB10B and BC20A; Fig. 2) are ca. 1.00 Ga, it is not likely that the ca. 800 Ma zircons in sample BB12A represent xenocrystic grains. Furthermore, considering that the rock is deformed and metamorphosed together with the host schists, we interpret that the dyke intruded the Brusque Complex protolith prior to the onset of orogenic evolution at ca. 650 Ma. Due to issues with stratigraphy, there is no constraint on what level of the Brusque Complex basin is represented by these metasediments, though it suggests that at least part of the Brusque Complex protolith was deposited prior to ca. 811 Ma.

This age is close to estimates of earliest sedimentation in the Porongos Complex of the central Dom Feliciano Belt foreland, which has been constrained to ca. 810–770 Ma by dating of syn-depositional volcanics (Pertille et al., 2017; Saalmann et al., 2011). These ages also correlate well with ca. 820–785 Ma syn-sedimentary magmatism in the Coastal Terrane of the Kaoko Belt hinterland (Konopásek et al., 2008, 2018), ca. 800 Ma magmatism in the Porto Belo Complex of the northern Dom Feliciano Belt hinterland (De Toni et al., 2020a), and ca. 790 Ma magmatism in the Várzea do Capivarita Complex of the central Dom Feliciano Belt hinterland (Martil et al., 2017), suggesting a genetic relationship between the early Neoproterozoic rocks of the foreland and hinterland domains (e.g. Battisti et al., 2018). Importantly, the dyke post-dates estimates for the beginning of continental rifting, and thus basin formation, in the Kaoko–Dom Feliciano–Gariep orogenic system at ca. 840 Ma (Basei et al., 2008b; Frimmel et al., 2001). All these data constrain the beginning of sedimentation in the Brusque Complex to between ca. 840–811 Ma.

None of the other potential metaigneous samples (BA22, JBE41B and JBE37) produced a cluster of dates that could be interpreted as a magmatic age. Thus, the ca. 811 Ma age obtained from sample BB12A provides the current best constraint for the minimum age of sedimentation of the Brusque Complex protolith.

4.2. Detrital zircon age patterns

Three distinct detrital zircon age patterns are identified within the studied samples (Fig. 7a). Sample BA22 contained too few zircons to confidently assign to a group, and so is not included in any further analysis.

The first pattern shows a polymodal age distribution, as seen in samples BB10B, BC20A, BB14A and JBE41B (Fig. 7b). These samples have age peaks predominantly within a range from ca. 2.10 to 1.00 Ga (Fig. 7b), with major Paleoproterozoic peaks at ca. 2.10, 1.95 and 1.80 Ga, and a series of peaks in the Mesoproterozoic at ca. 1.55, 1.35 and 1.20 Ga. Using the *1-O* parameter of Andersen et al. (2016) to statistically determine likeness between samples, samples BC20A, BB10B and JBE41B all show a perfect match within the sample confidence intervals (*1-O* = 0.00 for each comparison), and sample BB14A matches poorly with each (*1-O* = 0.11 for each comparison).

The next is a unimodal distribution pattern seen in samples BA23, BB22 and JBE37. The data show detrital zircon ages almost entirely within the Paleoproterozoic, and the pooled KDE (Fig. 7c) is dominated by a large, narrow peak at 2.20 Ga, with a series of smaller peaks between ca. 2.15–2.00 Ga. Sample JBE37 shows a good match with samples BA23 and BB22 (*1-O* = 0.03 and 0.02 respectively), and sample BA23 matches well with BB22 (*1-O* = 0.05). The pooled data do not show a strictly unimodal distribution pattern, but individually the samples show generally unimodal distributions (Fig. 5-c, 6-c, -g). The most noticeable difference when comparing the polymodal and the unimodal sample groups is the complete absence of Mesoproterozoic zircon age peaks in the latter, and the absence of a 2.20 Ga peak in the former.

Finally, an approximately bimodal distribution pattern is seen in samples JBD24 and BB08, and when these samples are pooled (Fig. 7d) the data show significant peaks at ca. 665 Ma and ca. 2.20 Ga, a minor peak at ca. 560 Ma, and individual dates distributed between ca. 2.10–0.80 Ga and between ca. 3.50–2.30 Ga. These two samples match perfectly within their confidence intervals (*1-O* = 0.00).

4.3. Polymodal detrital zircon pattern and its possible sources

When pooled, the major peaks in the polymodal pattern at ca. 2.10, 1.95, 1.80, 1.55, 1.35 and 1.20 Ga are distinct (Fig. 7b). Notably, there is no peak at 2.20 Ga, which is the dominant Paleoproterozoic age peak seen in the unimodal and bimodal pooled relative frequency plots (Fig. 7c and d). The oldest peaks in the pooled polymodal plot are at ca. 2.10 and 2.00 Ga, which correlate with magmatic ages of ca. 2.05–1.95 Ga from the Congo Craton basement of the Kaoko Belt (Kröner et al., 2004), as well as with similar ages reported from basement rocks of the Luis Alves Craton (Basei et al., 1999, 2009) and the Camboriú Complex (Silva et al., 2000). As the most proximal cratonic basement rocks to the Brusque Complex, the Luis Alves Craton would be the most likely candidate for protosource material for the Brusque Complex sediments. However, the absence of a ca. 2.20 Ga age peak suggests a closer affinity to the Congo Craton basement, which, unlike the Luis Alves Craton, does not contain a record of ca. 2.20 Ga activity.

The presence of Mesoproterozoic zircon grains in the polymodal

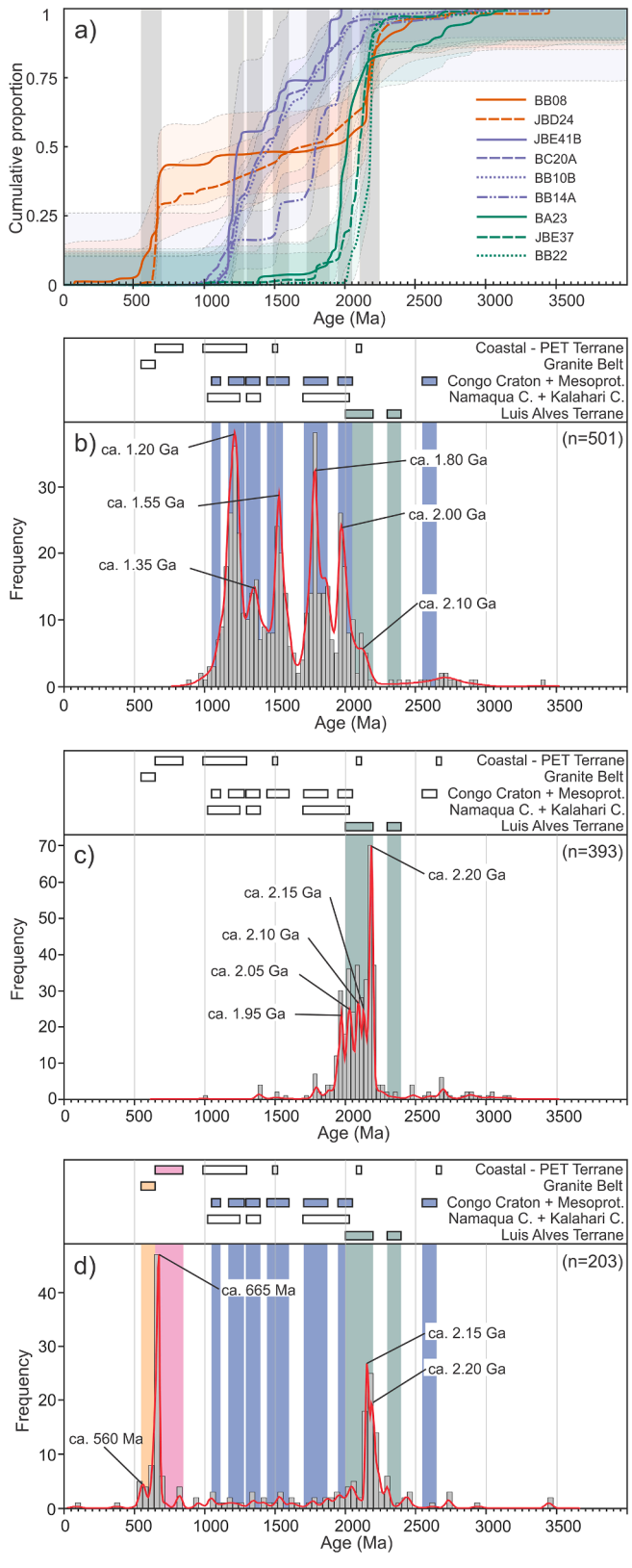

(caption on next column)

Fig. 7. Brusque Complex U–Pb detrital zircon data grouped into three patterns: a) cumulative proportion curves of each sample with 95% confidence intervals (shaded columns delineate major common age fractions), b) pooled polymodal group (samples BC20A, BB10B, BB14A and JBE41B), c) unimodal group (samples BA23, BB22 and JBE37), and d) bimodal group (samples BB08 and JBD24). Bars at the top of figures b, c and d show age ranges of relevant protosources, and the coloured columns behind the data show the best fit protosources for each group that correlate to major age fractions. Data for reference bars: Congo Craton + Mesoprot. from Kröner et al. (2015, 2004); Kröner and Rojas-Agramonte (2017); Seth et al. (1998, 2003), Namaqua Metamorphic Complex from Becker et al. (2006); Bial et al. (2015); Clifford et al. (2004), Luis Alves Craton from Basei et al. (2009); (Hartmann et al., 1999); Hartmann et al. (2000), Coastal–PET Terrane from Basei et al. (2011c); Goscombe et al. (2005a); Konopásek et al. (2008); Lenz et al. (2011); Oyhantçabal et al. (2009), Granite Belt from Florisbal et al. (2012b); Lara et al. (2020); Philipp and Machado (2005).

sample group indicates a significant contribution from Mesoproterozoic-aged protosource rocks, which were otherwise almost entirely absent during sedimentation of the protoliths of the unimodal sample group. However, rocks of this age are so far unknown from the basement rocks exposed in the northern Dom Feliciano Belt. In the southern Dom Feliciano Belt (Fig. 1), rocks with ages corresponding to the Mesoproterozoic peaks in the polymodal pattern, at ca. 1.50 and 1.40 Ga, are known only from the Nico Pérez Terrane in Uruguay (Gaucher et al., 2011; Mallmann et al., 2007; Oriolo et al., 2019; Oyhantçabal et al., 2018; Sánchez-Bettucci et al., 2004). A ca. 1.55 Ga crystallisation age is also recorded within the Capivarita Anorthosite in the exposed basement of the Granite Belt in the central part of the Dom Feliciano Belt in Rio Grande do Sul (Chemale et al., 2011). Given their distal nature to the northern Dom Feliciano Belt, though, it is unlikely that these rocks directly contributed to sedimentation into the Brusque Complex paleobasin.

The 1.55–1.40 Ga ages are common, however, in Mesoproterozoic magmatic rocks intruding the Congo Craton of Namibia and SW Angola (e.g. Bybee et al., 2019; Lehmann et al., 2020; Luft et al., 2011; Seth et al., 1998), providing possible protosources for the Brusque Complex sediment. The best-fit source rocks for the observed ages in the polymodal group come from metamorphosed supracrustal rocks of the Okapuka Formation and the underlying Epupa Metamorphic Complex in the Kaoko Belt (Fig. 7b). Part of the Congo Craton, the Epupa Metamorphic Complex is dated at ca. 1.85–1.75 Ga (Kröner et al., 2010, 2015), and is intruded by granitoid rocks with ages primarily clustered at ca. 1.50, 1.35 and 1.20 Ga (Drüppel et al., 2007; Kröner et al., 2015; Kröner and Rojas-Agramonte, 2017; Seth et al., 2003). These basement rocks are overlain by the ca. 1.35 Ga volcano-sedimentary Okapuka Formation (Fig. 1), which contains detrital zircon spanning ca. 2.05–1.40 Ga that was likely sourced from the nearby basement. The formation is intruded by magmatic rocks with ages between ca. 1.20–1.05 Ga (Kröner and Rojas-Agramonte, 2017).

The underlying Paleoproterozoic basement may represent part of the source for the Brusque Complex sediments, however it is equally likely that these rocks represent the protosource and that the Brusque Complex sediment is sourced directly from the Mesoproterozoic sedimentary cover (Okapuka Fm.) and associated intrusive rocks. Recycling of older sedimentary successions has been proposed by Andersen et al. (2018a) to explain the detrital zircon record in equivalent rocks in the Gariep Belt, and they point to preserved fragments of Meso- and Paleoproterozoic sedimentary cover on the surrounding cratonic basement as evidence of this recycling system. Similarly, Konopásek et al. (2017) and Konopásek et al. (2018) inferred an extensive Mesoproterozoic sedimentary cover sequence as the source for the Neoproterozoic successions of the Kaoko Belt foreland. Given the presumed pre-Atlantic proximity of the Kaoko Belt to the northern Dom Feliciano Belt (Konopásek et al., 2017; Porada, 1989), we judge this inferred extensive Mesoproterozoic cover sequence as the most likely candidate for the

Mesoproterozoic zircon populations in the Brusque Complex rocks.

4.4. Unimodal detrital zircon pattern and its possible sources

Zircon ages at ca. 2.20 Ga, corresponding to the largest peak in the unimodal pooled zircon age distribution pattern (Fig. 7c), are known from local basement rocks of the Luis Alves Craton, the Camboriú Complex and the Águas Mornas Complex (Basei et al., 2009; Hartmann et al., 1999, 2000; Silva et al., 2000, 2005). The closest basement unit of the Luis Alves Craton is the Santa Catarina Granulite Complex, which outcrops immediately to the north of the Itajaí Basin (Fig. 1). Zircon grains from granulitic gneisses of this complex mostly preserve U–Pb ages of ca. 2.20–2.10 Ga, with less common ca. 2.40–2.30 Ga ages and minor occurrences of ca. 2.00 Ga zircon (Basei et al., 2009; Hartmann et al., 1999, 2000). Ages corresponding to the smaller peaks at ca. 2.10 and 2.00 Ga are also known from the Camboriú Complex (Silva et al., 2000, 2005), as well as from exposed Congo Craton basement in the Kaoko Belt (Kröner et al., 2004). As the samples from the unimodal group contain only single zircon age peaks, which correspond to ages in the local basement, we interpret the unimodal group as reflecting first generation detrital zircon and thus direct erosion of the basement.

The Brusque Complex contains both local basement-derived sediment and recycled sediment, however the absence of a 2.20 Ga age peak in the polymodal group suggests that these two sources did not mix. This indicates that the inferred Mesoproterozoic sedimentary cover source was completely eroded before any of the local basement was exposed. Inferring from this that the sediment was sourced locally implies also that the Mesoproterozoic sedimentary sequences covered the Luis Alves basement prior to erosion into the Brusque Complex paleobasin, and thus that the Congo and Luis Alves cratons were in close proximity prior to Neoproterozoic rifting.

Both the unimodal and polymodal sample groups do not contain zircon age peaks younger than 1.20 Ga, and even the youngest individual zircons are no older than ca. 0.9–1.0 Ga (Fig. 7b and c). Considering the minimum age of sedimentation at ca. 810 Ma, the Brusque Complex metasediments therefore contain no zircon grains sourced from syn-sedimentary igneous rocks. This is typical of rift basin or passive margin environments, where the influx of material into the basin is dominated by older grains sourced from the surrounding craton (Cawood et al., 2012).

4.5. Bimodal detrital zircon pattern and its possible sources

The two samples with bimodal age distribution contain the youngest zircon grains of all the studied samples, with between one third and one half of the total analysed grains dated in the Neoproterozoic. Using the youngest zircon age peak as a conservative estimate of the timing of sedimentation (Dickinson and Gehrels, 2009), the maximum age of sedimentation of the protolith is ca. 560 Ma (Fig. 7d). However, the much more robust peak at ca. 665 Ma is a safer benchmark for the maximum sedimentation age, considering the possibility of lead loss in the small number of younger grains during late-stage orogenic deformation or modern weathering. This post-dates the ca. 811 Ma minimum age of sedimentation constrained in this study by at least ca. 150 million years, implying the presence of two temporally distinct sedimentary protoliths. This observation remains difficult to confirm in the field, as the younger rocks appear to be metamorphosed at similar greenschist facies conditions as the low-grade Brusque Complex rocks, and they exhibit a deformation style indistinguishable from the high-strain zones of the Brusque Complex further inland (see Basei et al., 2011b). Indeed, it is possible that ancient lead loss could account for the Neoproterozoic zircon peaks by skewing Mesoproterozoic ages along the concordia towards younger values (e.g. Andersen et al., 2019). However, the large Neoproterozoic fraction (up to ca. 45%), the low-grade metamorphic conditions, and the remarkable similarity of the detrital signature to that of the adjacent Itajaí Basin (see section 4.6) favours the former interpretation. Further, two distinct depositional episodes have also recently been identified in the Porongos Complex of the central Dom Feliciano Belt foreland (Battisti et al., 2018; Höfig et al., 2018).

The ca. 2.20 Ga age peak and the spread of individual Mesoproterozoic and Paleoproterozoic dates between ca. 2.10–1.00 Ga (Fig. 7d) show similarities with the unimodal and polymodal groups respectively (Fig. 7b and c). The ca. 665 Ma age fits well with earliest estimates of the timing of orogenesis in the Dom Feliciano Belt (De Toni et al., 2020b), and thus the most likely protosource for the ca. 665 peak is the orogenic hinterland. The hinterland rocks record ca. 650–645 Ma zircon ages (Chemale et al., 2012) associated with orogenesis in the northern Dom Feliciano Belt, and up to ca. 665–660 Ma (Frantz et al., 2003; Masquelin et al., 2012) in the southern Dom Feliciano Belt. The number of grains between ca. 640–600 Ma fit with known ages from the Granite Belt, which intruded the orogenic hinterland between ca. 640–580 Ma (Chemale et al., 2012; Florisbal et al., 2012b).

Considering this possible protosource, the distribution pattern shown in Fig. 7d can thus be explained by a combination of recycled (meta) sedimentary rocks with a detrital zircon content matching the unimodal and polymodal sample groups of the Brusque Complex, and syn-orogenic rocks sourced directly from the orogenic hinterland.

4.6. Comparison with the Itajaí basin

The data suggest that the sedimentary protoliths of the bimodal sample group were sourced from erosion of the rising orogen, and thus they possibly represent syn-orogenic flysch- or molasse-type sediments similar to the Itajaí Basin. In support of this, the data from the Itajaí Basin show remarkably similar detrital zircon patterns, with the same primary age fractions with major peaks at ca. 650–550 Ma and

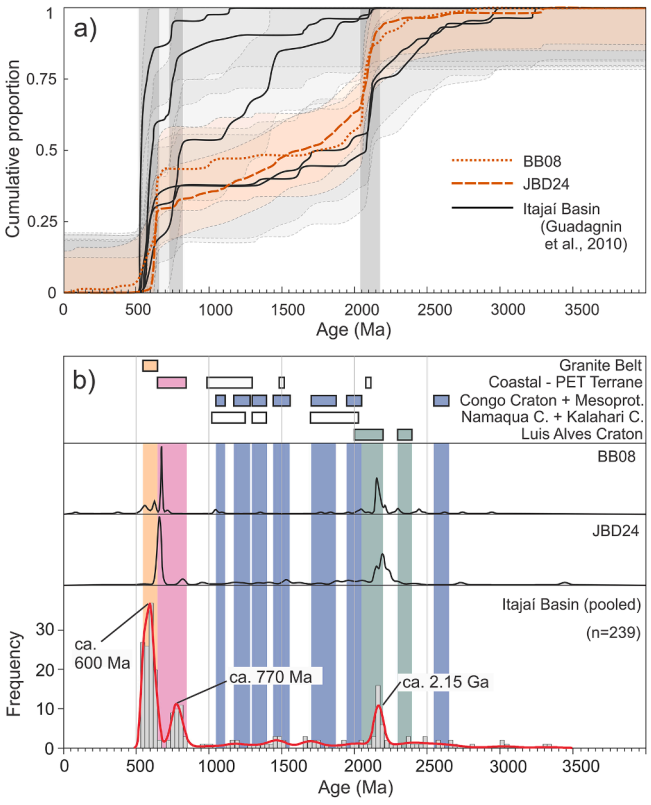

Fig. 8. Comparison between detrital zircon signatures of samples BB08, JBD24, and the Itajaí Basin: a) individual cumulative distribution curves with 95% confidence intervals (shaded columns delineate major common age fractions) b) KDEs and frequency histograms, with pooled Itajaí Basin data. Data for Itajaí Basin from Guadagnin et al. (2010). See Fig. 7 for age range references.

2.20–2.05 Ga, and a distribution of individual ages between ca. 2.00–1.00 Ga (Fig. 8a and b). Further, the ages corresponding to the small peak at ca. 560 Ma in the KDE curve are known from syn-sedimentary volcanism in the Itajaí Basin (Guadagnin et al., 2010), although the small number of grains younger than 600 Ma (8 grains) make this correlation only speculative.

The Itajaí Basin shows a typical orogenic foreland deformation style (e.g. Condie, 2016), with the margin closest to the foreland fold and thrust belt (i.e. the Schist Belt) showing stronger deformation than the opposite margin (Basei et al., 1998b; Guadagnin et al., 2010). Given the proposed source rocks and similarities with the Itajaí Basin sediments, we interpret samples JBD24 and BB08 as belonging to syn-orogenic sediments deposited in a foreland basin setting similar to the Itajaí Basin, or possibly part of the Itajaí Basin itself. The proximity and structural correlation of these rocks to the Itajaí–Perimbó Shear Zone (Fig. 2) lends support to this interpretation, as parts of the foreland basin closest to the leading edge of the fold-and-thrust belt would likely become tectonically interleaved with the Brusque Complex, making the deformation history between the two distinct protoliths indistinguishable.

4.7. Comparing the Kaoko–Dom Feliciano–Gariep Neoproterozoic foreland units

The Brusque Complex zircon distribution shares many similarities with the foreland fold-and-thrust belt cover sequences of the central Dom Feliciano Belt (Porongos Complex), the Kaoko Belt and the Gariep Belt. Fig. 9 compares detrital zircon data from these four regions, showing pooled data from various published detrital zircon studies (Andersen et al., 2018a; Gruber et al., 2011; Höfig et al., 2018; Hofmann et al., 2014; Konopásek et al., 2014, 2017; Pertille et al., 2015a, 2017), with samples grouped together based on the patterns as recognized in this study. The same two detrital zircon age distribution patterns as seen in the Brusque Complex are recorded in each of the other regions, with only minor differences (Fig. 9a and b). The Lavalleja Complex in Uruguay is often interpreted as the continuation of the Schist Belt in the southern Dom Feliciano Belt (Basei et al., 2008a). However, due to the small number of published detrital zircon datasets and poor age constraints (see Hueck et al., 2018b), the potential correlation of the Lavalleja Complex with the rest of the Schist Belt will not be further discussed.

The pooled polymodal group of the Porongos Complex samples matches well with the Brusque Complex rocks of this study (Fig. 9a and c). Using the *1-O* parameter of Andersen et al. (2016), they show a perfect pairwise overlap within 95% confidence intervals (*1-O* = 0.00). Like the Brusque Complex, the pooled data of the Porongos Complex is missing a 2.20 Ga peak, suggesting a majority African affinity for the sedimentary protosources (Fig. 9c). The similarities between the units imply that they shared the same source, which supports the interpretation that the Schist Belt of the Dom Feliciano Belt represents sediment deposited into a coeval and spatially related system of paleobasins.

The Porongos Complex unimodal group also shows a good match with the equivalent Brusque Complex rocks (Fig. 9b) (pairwise overlap *1-O* = 0.04). The Paleoproterozoic peaks between ca. 2.20–2.00 Ga in the samples with unimodal distribution have been linked with local basement rocks of the Encantadas Complex (Pertille et al., 2015a, 2017), and can also be correlated with ca. 2.50–2.00 Ga basement rocks of the Taquarembó Block, part of the Nico Pérez Terrane (Fig. 9d) (Oyhantçabal et al., 2011b, 2018 and references therein). The similarities in age between the Brazilian Nico Pérez Terrane (Taquarembó Block) and the Luis Alves Craton, most notably the presence of ca. 2.20 Ga rocks which are absent on the African side of the orogen, suggests that these cratonic blocks may represent a continuous basement unit.

For the Kaoko Belt, the two sample groups are pooled based on the patterns as recognised in this study and as constrained by the local stratigraphy (Fig. 9b and c) (Konopásek et al., 2014, 2017). Konopásek et al. (2017) showed that the pre-orogenic stratigraphic position of the Kaoko Belt metasedimentary rocks can be distinguished based on their detrital zircon signatures, with the lower sequences containing both Paleoproterozoic and Mesoproterozoic ages, and the upper sequences dominated by Paleoproterozoic ages only. The Kaoko Belt polymodal group shows strong similarities to the Brusque and Porongos Complexes (Fig. 9a) (pairwise overlap *1-O* = 0.03 and 0.02 respectively). The Mesoproterozoic peaks at ca. 1.55, 1.40 and 1.20 Ga match well with those from the Brusque Complex, and the same with the Paleoproterozoic peaks between ca. 2.10–1.80 Ga and the notable absence of ca. 2.20 Ga zircon. The only significant difference between the Mesoproterozoic detrital signals of the Kaoko and Dom Feliciano Belts is the presence of a ca. 1.05 Ga peak in the Kaoko Belt rocks (Fig. 9c), which can also be found in the foreland supra-crustal rocks of the Gariep Belt (Basei et al., 2005; Hofmann et al., 2014, 2015).

The pooled unimodal group shows a prominent Paleoproterozoic peak similar to the Brusque and Porongos complexes (Fig. 9d). However, the peak is centred at 1.80 Ga, resulting in a poor pairwise overlap comparison (Fig. 9b) (*1-O* = 0.11). This age peak fits with erosion of the local Congo Craton basement (Kröner et al., 2004; Luft et al., 2011).

Konopásek et al. (2017) recognised the gradual disappearance of Mesoproterozoic zircon from the upper parts of the Kaoko Belt supracrustal sequences, and suggested that this reflects the complete erosion of Mesoproterozoic supracrustal source rocks into the lower parts of the paleobasin, with the upper sequences representing erosion of the exposed local basement. Given evident similarities in detrital zircon signatures, it is possible that the Brusque Complex protolith was deposited in the same way; the rocks with polymodal zircon distribution representing the lower strata, and those with unimodal distribution the upper strata of the basin. This interpretation would necessitate a complete revision of the current stratigraphy of the Brusque Complex (Basei et al., 2006, 2011b), as the samples with polymodal and unimodal patterns come from all known stratigraphic levels. However, given problems with exposure in the northern Dom Feliciano Belt, it remains difficult to test this hypothesis, and is otherwise beyond the scope of this study.

Data from the Port Nolloth Zone of the Gariep Belt (Andersen et al., 2018a; Hofmann et al., 2014) also fit into unimodal and polymodal groups (Fig. 9 a and b). The polymodal group contains the same late Mesoproterozoic age peaks at ca. 1.30, 1.20 and 1.10 Ga (Fig. 9c), however there is a conspicuous absence of early Mesoproterozoic ages ca. 1.50 Ga, resulting in poor pairwise overlap comparisons (*1-O*: Brusque Complex = 0.18, Porongos Complex = 0.22, Kaoko Belt = 0.22). The Namaqua Metamorphic Complex outcropping along the western edge of the Kalahari Craton contains abundant Mesoproterozoic rocks dated between ca. 1.30–1.00 Ga (Becker et al., 2006; Bial et al., 2015; Clifford et al., 2004), and has no record of 1.50 Ga events, making these rocks the most likely protosource. The Gariep unimodal group is dominated by a single Paleoproterozoic peak at 1.90 Ga, which fits with basement of the Kalahari Craton (Fig. 9d) and closely matches the Kaoko Belt unimodal group (pairwise overlap *1-O* = 0.04). Andersen et al. (2018a) interpret the Gariep Belt detrital zircon signature as the result of mixing of various protosources during sedimentary recycling events prior to Neoproterozoic rifting, similar to the inferred Mesoproterozoic sedimentary cover of Konopásek et al. (2017). However, the differences between the Gariep Belt and the rest of the orogen clearly shows there is local variation in the recycled sediment protosources,

The similarities in detrital signatures strongly suggest that the pre-orogenic supracrustal rocks of the Brusque Complex, Porongos Complex and the Kaoko Belt partly shared the same source, and that the Gariep Belt shared at least some of the same protosources. The protosources for the polymodal group are clearly of African affinity, with no clear equivalent in the South American rock record, suggesting that the sediment was sourced from Mesoproterozoic (volcano-)sedimentary sequences containing recycled African detritus.

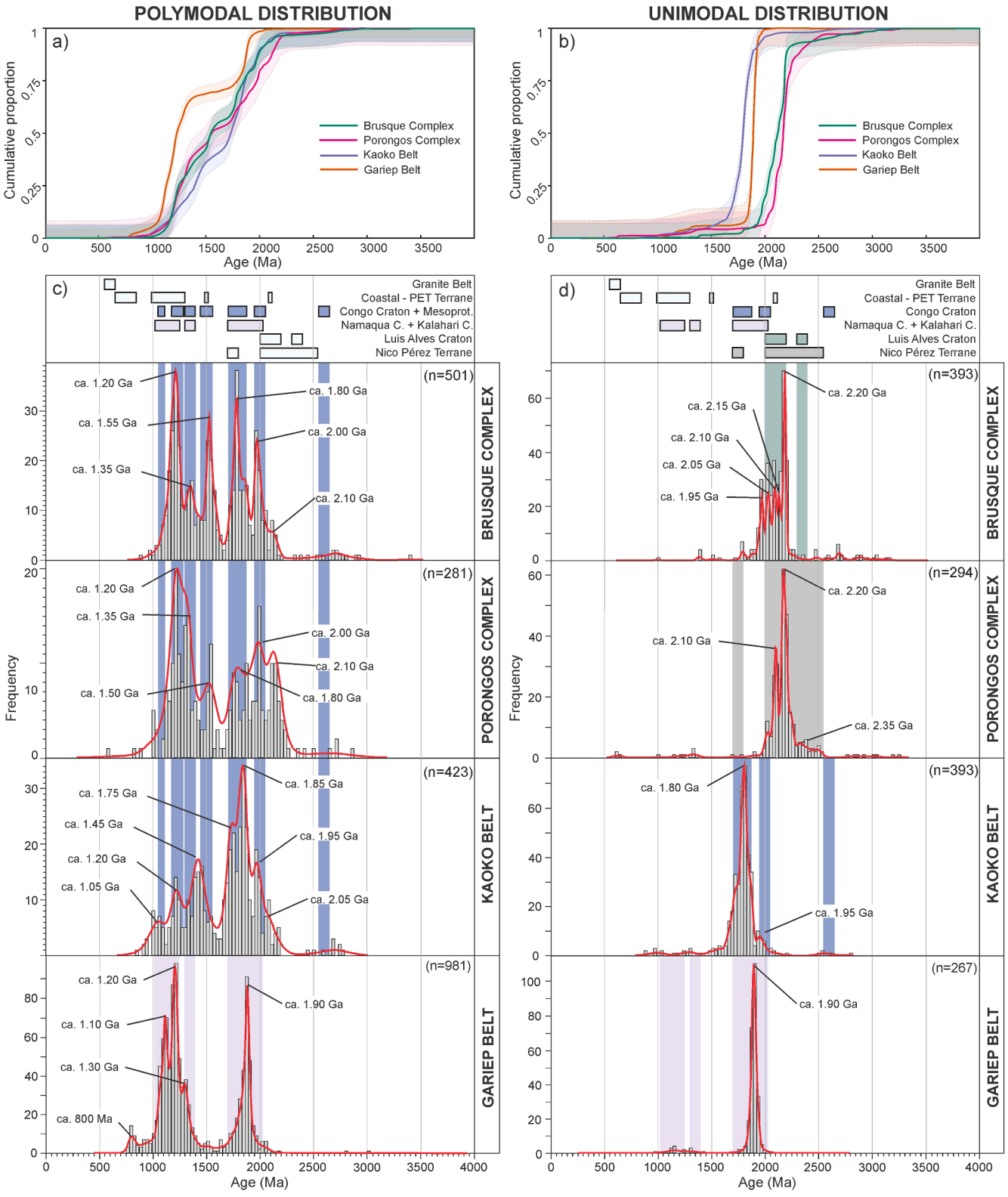

Fig. 9. Comparison between detrital zircon data of the pre-orogenic metasediments of the Brusque Complex, the Porongos Complex, the Kaoko Belt and the Gariep Belt (Porth Nolloth Zone): a) cumulative distribution curves for pooled polymodal group, b) cumulative distribution curves for pooled unimodal group, c) KDEs and histograms for polymodal group and d) KDEs and histograms for unimodal group. Data are grouped according to the patterns as identified in this study. Data sources: Brusque Complex from this study, Porongos Complex from Gruber et al. (2011); Höfig et al. (2018); Pertille et al. (2015a, 2015b, 2017), Kaoko Belt from Konopásek et al. (2014, 2017), Gariep Belt from Andersen et al. (2018a); Hofmann et al. (2014). Nico Pérez age range from Oyhantçabal et al. (2018) and references therein. See Fig. 7 for references for the remaining age-range bars.

4.8. Tectonic setting and evolution of the Schist Belt

Fig. 10 shows schematic cross sections across the northern Dom Feliciano Belt and the Kaoko Belt, outlining the proposed evolution of the Schist Belt as inferred from the Brusque Complex U–Pb zircon data and correlations with the other units. During the pre-rifting stage at ca. 1.0 Ga–850 Ma, the Congo and Luis Alves cratons were connected, accompanied by Mesoproterozoic terranes and cover sequences associated with the amalgamation of Rodinia (Fig. 10a) (Bial et al., 2015; Miller, 2012). The lack of detrital zircon close to the age of

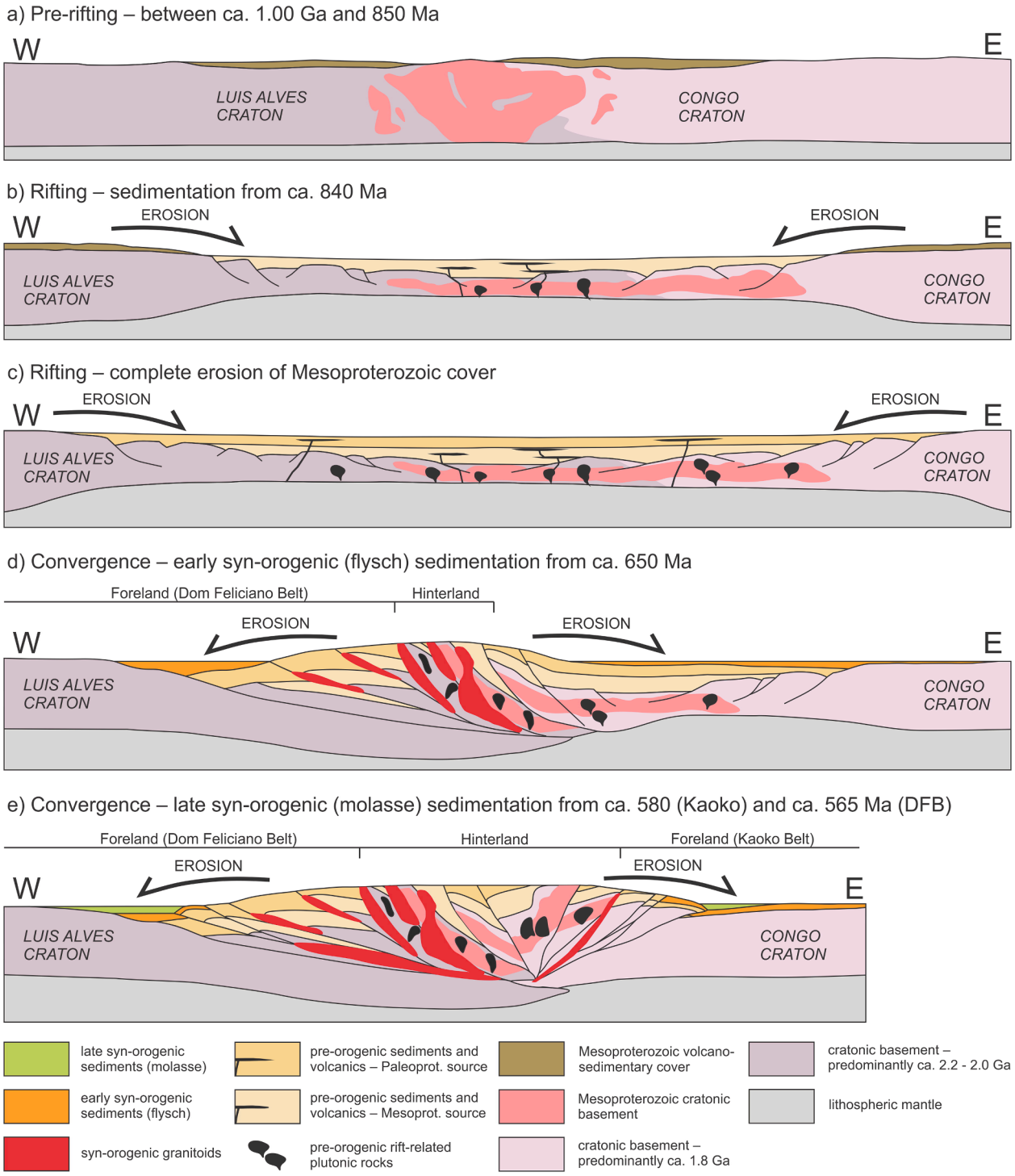

Fig. 10. Schematic cross sections outlining the proposed evolution of the Kaoko–Dom Feliciano Belt as inferred from U–Pb detrital zircon data: a) pre-rifting stage ca. 1.0 Ga–850 Ma, the Congo and Luis Alves cratons are connected, together with Mesoproterozoic terranes and cover sequences associated with Rodinia amalgamation, b) rifting from ca. 840 Ma, erosion of an extensive Mesoproterozoic cover sequence, sedimentation into the rift basin from at least ca. 810 Ma, c) rifting continues, complete erosion of the Mesoproterozoic cover and erosion of the Luis Alves and Congo Craton Basement, d) rift inversion and convergence leads to orogenesis at ca. 650, and the erosion of the rising hinterland leads to sedimentation (flysch) into *syn*-orogenic basins, e) continued convergence leads to the movement of the orogenic front towards the east and the formation of the Kaoko Belt, more sedimentation into both foreland basins, and late deformation in the west leads to deformation and metamorphism of the *syn*-orogenic sediments in the Brusque Complex.

sedimentation within the pre-orogenic sediments of the Kaoko–Dom Feliciano–Gariep Belt indicates the absence of magmatic activity on the crust of either basin margin at this time. Based on the model of Cawood et al. (2012), the pre-orogenic sediments of the Brusque Complex, Porongos Complex, Kaoko Belt and Gariep Belt best fit into an extensional setting, as the youngest 5% of zircon are>150 m.y. older than the age of sedimentation (Fig. 11). This finding supports a pure intracontinental rifting model for the formation of the Kaoko–Dom Feliciano–Gariep basin (Konopásek et al., 2018, 2020), and is in disagreement with various proposed subduction-collision models that place arc-magmatism inside and/or at the margin of the basin during or before its opening (De Toni et al., 2020a; Koester et al., 2016; Lenz et al., 2013; Martil et al., 2017). Based on this interpretation, the basin formed by intracontinental rifting from ca. 840 Ma (Basei et al., 2008b), with sedimentation into the Brusque Complex paleobasin from at least ca. 810 Ma (Fig. 10b). The complete erosion of the Mesoproterozoic cover sequences on the South American side, and the near-complete erosion on the African side, led to erosion of the Luis Alves and Congo cratons into the rift basin (Fig. 10c).

The period prior to convergence and orogenesis consisted of either 1) rift-drift transition and the development of the Adamastor Ocean (e.g. Basei et al., 2018 and references therein), or 2) continued intracontinental rifting and little to no oceanic spreading (e.g. Konopásek et al., 2020). Due to the continued lack of geochronological constraints on sedimentation into the Brusque Complex paleobasin, the duration of rifting cannot be inferred from our data. However, based on the lack of evidence of late-Neoproterozoic subduction-related metamorphism, the syn- to post- collisional nature of the Granite Belt (Bitencourt and Nardi, 1993, 2000; Florisbal et al., 2012a, 2012b), and evidence in the Kaoko Belt of crustal stretching and sedimentation up to ca. 660 Ma (Konopásek et al., 2020), the latter model is favoured for this interpretation.

Based on similarities with the Itajaí Basin, we interpret the syn-orogenic sediments of the Brusque Complex as belonging to a collisional foreland setting (Fig. 11). This suggests that, after rift inversion and convergence led to orogenesis at ca. 650 Ma (De Toni et al., 2020b), the eroding rising hinterland fed into proximal syn-orogenic basins (Fig. 10d). Finally, continued convergence led to the movement of the orogenic front towards the east (Fig. 10e), where the hinterland overrode the Congo Craton margin and led to the development of the Kaoko Belt from ca. 580 Ma (Goscombe et al., 2003a; Konopásek et al., 2008). This late-stage convergence is reflected in the northern Dom Feliciano belt by the deformation of syn-orogenic sediments and their possible incorporation into the Brusque Complex (Fig. 10e).

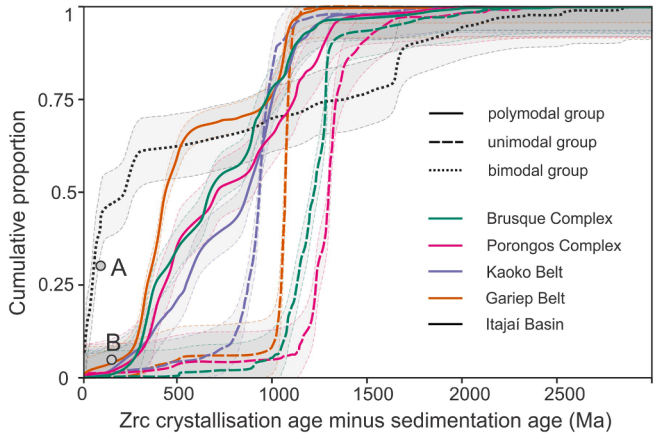

Fig. 11. Summary cumulative distribution function plot (with 95% confidence intervals) showing the difference between the detrital zircon crystallisation age and the sedimentation age of the various sample groups in this study. Point A and B are from Cawood et al. (2012), showing the points used to predict tectonic setting: A–youngest 30% of grains with < 100 M.y. difference suggests convergent tectonic setting, >100 M.y. difference suggests collisional foreland setting; B–youngest 5% of grains with < 150 M.y. difference suggests collisional foreland setting, >150 M.y. difference suggests extensional setting. Sedimentation ages are based on this study and from other sources in the text.

4.9. Tectonic implications for pre-orogenic configuration

Based on pre-Atlantic plate reconstructions (Heine et al., 2013), and correlations between basement units (Konopásek et al., 2016), the Brusque Complex and Kaoko Belt foreland fold-and-thrust belts were located at approximately similar positions on either side of the orogenic hinterland (Fig. 12). The identification of a single source for significant parts of the pre-orogenic supracrustal rocks of the Dom Feliciano and Kaoko belts provides strong evidence to also correlate these rocks prior to early-Neoproterozoic rifting. Considering their deposition into a system of coeval, spatially related paleobasins, the Congo Craton, Luis Alves Craton and Nico Pérez Terrane must have been in close proximity at the onset of early-Neoproterozoic rifting (Fig. 10). Despite differences in protosources, the similarities in sedimentation history of the Gariep Belt suggests the involvement of the Kalahari Craton as well.

This means that, considering the correlation between the northern and central parts of the Schist Belt (Fig. 12), the rifting stage beginning at ca. 840–830 Ma (Basei et al., 2008b; Frimmel et al., 2001) may have involved a combined Luis Alves – Nico Pérez terrane rifting from the Congo and Kalahari cratons (Johansson, 2014; Konopásek et al., 2018). Although some authors argue that these cratonic fragments were separated by wide oceanic domains at the time of sedimentation (e.g. Foster et al., 2015), the data from this study support tectonic models that place these crustal blocks together in Rodinia at the onset of rifting (e.g. Konopásek et al., 2020; Oriolo et al., 2016; Oyhantçabal et al., 2011a; Philipp et al., 2016; Rapela et al., 2011).

The results of this study also contradict suggestions that the Major Gercino Shear Zone, and possibly the rest of the Southern Brazilian Shear Belt, separates distinct sedimentary rocks of African affinity on one side, and South American affinity on the other (Basei et al., 2000, 2008a). Although there are differences in source region for parts of the sedimentary protoliths that correlate with local African or South American basement, the Mesoproterozoic detrital zircon ages in both belts show a shared source with clear African affinity, and based on this study there is no indication that the Major Gercino Shear Zone represents a syn-sedimentary, pre-orogenic structure that separated basins with entirely different source regions.

5. Conclusions

1) U–Pb zircon dating of a felsic dyke intruding sedimentary rocks of the Brusque Complex constrains the minimum age of sedimentation into the Brusque Complex paleobasin at 811 ± 6 Ma. This age correlates with sedimentation age constraints in the Porongos Complex, Kaoko Belt and Gariep Belt, and with the age of pre-orogenic magmatism and sedimentation in the orogenic hinterland.
2) U–Pb detrital zircon dating of metamorphosed magmatic and sedimentary rocks of the Brusque Complex reveals three distinct sample groups. The first group shows a polymodal age distribution, with peaks in both the Meso- and Paleoproterozoic. The second group contains only Paleoproterozoic ages, dominated by a single age peak. The third group shows a mostly bimodal age distribution, with a major Neoproterozoic age fraction.
3) Potential protosources for the Mesoproterozoic zircon grains in the polymodal sample group are all of African affinity. The most likely source for the sediment was Mesoproterozoic sedimentary cover of the Congo Craton bearing recycled zircon grains. We suggest that the Mesoproterozoic sediment also covered the Luis Alves Craton prior to Neoproterozoic rifting. The Paleoproterozoic zircon grains from the unimodal sample group were likely sourced from local basement represented by the Luis Alves Craton and Camboriú Complex.

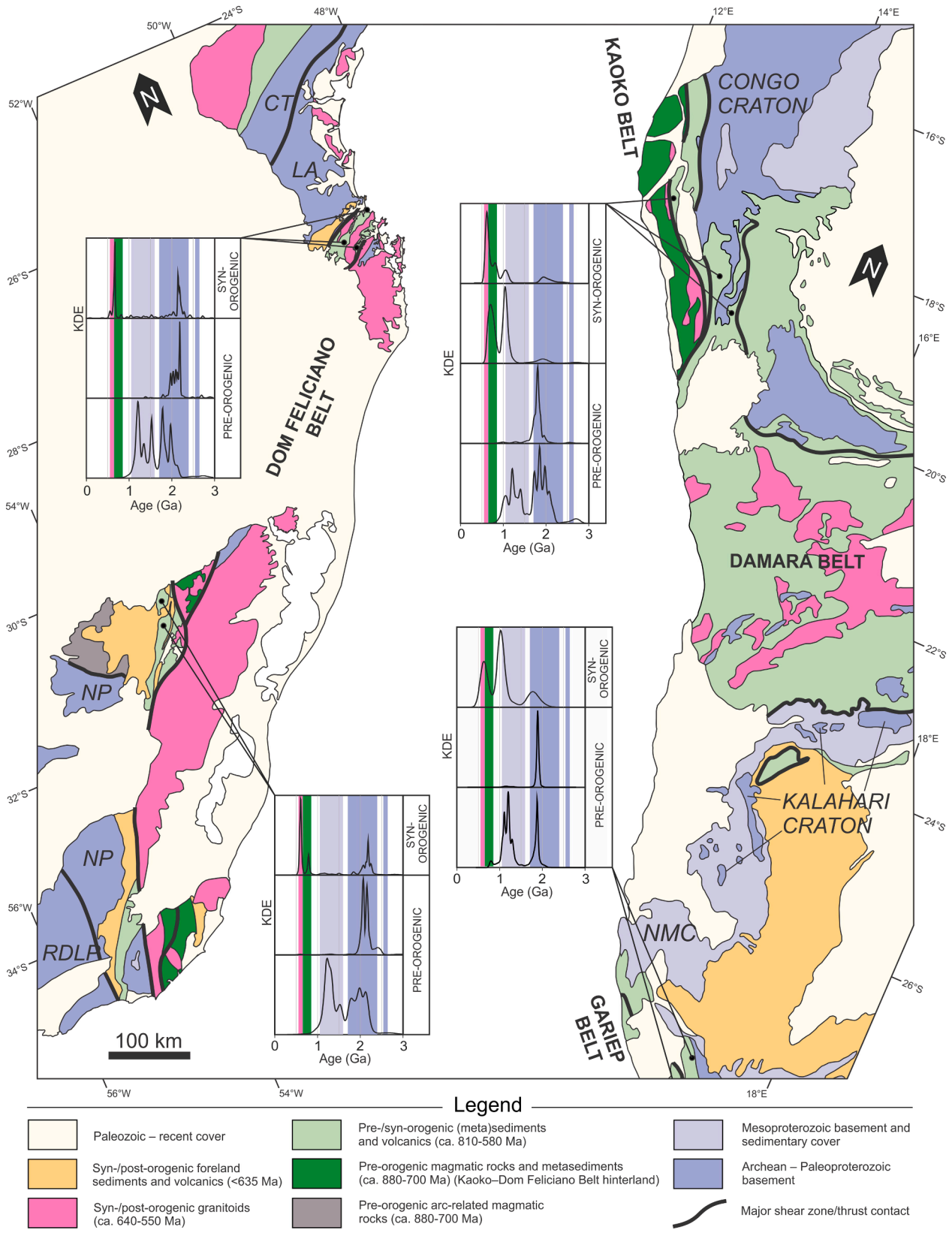

Fig. 12. Overview map showing the correlation of metasedimentary rocks of the Kaoko–Dom Feliciano Belt orogenic forelands (modified after Hueck et al., 2018b; Konopásek et al., 2017; McCourt et al., 2013; Oyhantçabal et al., 2011b; and Passarelli et al., 2018). NMC = Namaqua Metamorphic Complex, RDLP = Rio de la Plata Craton, NP = Nico Pérez Terrane, LA = Luis Alves Craton, CT = Curitiba Terrane. For KDE figures see Fig. 7 for references. Coloured bars behind KDE curves represent probable protosource regions, and the colours correspond to those regions as shown in the map.

4) The Neoproterozoic zircon grains in the bimodal sample group post-date sedimentation in the Brusque Complex paleobasin as constrained in this study, suggesting that these rocks belong to a later paleobasin formed in a different tectonic environment. Similarities with the Itajaí Basin suggest that they represent parts of a syn-orogenic foreland basin, with sediment sourced from the rising orogenic hinterland. The rocks were likely tectonically interleaved with the Brusque Complex during late-stage orogenic deformation.
5) The absence of Neoproterozoic zircon at or close to the age of sedimentation in the pre-orogenic sediments of the Brusque Complex implies that the paleobasin did not evolve within a convergent tectonic setting, supporting a pure intracontinental rifting model for basin formation.
6) Comparison of pre-orogenic Brusque Complex detrital zircon data with equivalent rocks in the Porongos Complex, Kaoko Belt and Gariep Belt indicates a shared source and/or shared basin evolution, implying that these sediments were deposited into a system of coeval and spatially related paleobasins. The data imply that the Luis Alves Craton, Congo Craton, Nico Pérez Terrane and Kalahari Craton were in close proximity at the start of Neoproterozoic rifting and the breakup of Rodinia.

CRediT authorship contribution statement

Jack James Percival: Conceptualization, Methodology, Formal analysis, Investigation, Writing - original draft, Visualization. **Jiří Konopásek:** Conceptualization, Methodology, Resources, Funding acquisition, Writing - review & editing, Project administration, Supervision. **Ragnhild Eiesland:** Conceptualization, Methodology, Formal analysis, Investigation. **Jiří Sláma:** Investigation, Formal analysis, Validation, Data curation. **Roberto Sacks de Campos:** Investigation, Writing - review & editing. **Matheus Ariel Battisti:** Investigation, Writing - review & editing. **Maria de Fátima Bitencourt:** Supervision, Writing - review & editing.

Declaration of Competing Interest

The authors declare that they have no known competing financial interests or personal relationships that could have appeared to influence the work reported in this paper.

Acknowledgements

This work was supported by the Norwegian Centre for International Cooperation in Education (SIU), the Norwegian Agency for International Cooperation and Quality Enhancement in Higher Education (Diku), and the Coordenação de Aperfeicoamento de Pessoal de Nível Superior (CAPES) in Brazil through the grant projects no. UTF-2016-CAPES-SIU10024 and UTF-2018-CAPES-Diku-10004. J. Konopásek acknowledges financial support of the Czech Science Foundation, grant no. 18-24281S. J. Sláma was supported by the ASCR institutional support RVO 67985831. Acknowledgements and thanks to D. Lyra for fieldwork assistance. The authors are grateful to T. Andersen and an anonymous reviewer for their helpful reviews.

Appendix A. Supplementary data

Supplementary data to this article can be found online at https://doi.org/10.1016/j.precamres.2020.106060.

References

Almeida, R.P., Janikian, L., Fragoso-Cesar, A.R.S., Fambrini, G.L., 2010. The Ediacaran to Cambrian Rift System of Southeastern South America: tectonic Implications. J. Geol. 118 (2), 145–161. https://www.doi.org/10.1086/649817.

Andersen, T., Elburg, M., Cawthorn-Blazeby, A., 2016. U-Pb and Lu–Hf zircon data in young sediments reflect sedimentary recycling in eastern South Africa. J. Geol. Soc. 173 (2), 337–351. https://doi.org/10.1144/jgs2015-006.

Andersen, T., Elburg, M.A., van Niekerk, H.S., Ueckermann, H., 2018a. Successive sedimentary recycling regimes in southwestern Gondwana: Evidence from detrital zircons in Neoproterozoic to Cambrian sedimentary rocks in southern Africa. Earth-Sci. Rev., vol. 181, pp. 43-60. Doi: 10.1016/j.earscirev.2018.04.001.

Andersen, T., Kristoffersen, M., Elburg, M.A., 2018b. Visualizing, interpreting and comparing detrital zircon age and Hf isotope data in basin analysis – a graphical approach. Basin Res., vol. 30, no. 1, pp. 132-147. Doi: 10.1111/bre.12245.

Andersen, T., Elburg, M.A., Magwaza, B.N., 2019. Sources of bias in detrital zircon geochronology: Discordance, concealed lead loss and common lead correction. Earth-Sci. Rev. 197, 102899 https://doi.org/10.1016/j.earscirev.2019.102899.

Basei, M.A.S., McReath, I., Siga Jr., O., 1998a. The Santa Catarina Granulite Complex of Southern Brazil: A Review. Gondwana Res. 1 (3–4), 383–391. https://www.doi.org/10.1016/S1342-937X(05)70854-6.

Basei, M.A.S., Citroni, S.B., Siga Jr, O., 1998b. Stratigraphy and age of fini-Proterozoic basins of Parana and Santa Catarina States, southern Brazil. Boletim IG-USP, Serie Cientifica 29, 195–216.

Basei, M.A.S., Siga, Jr O., Reis Neto, J.M.d., Passarelli, C.R., Prazeres, H., Kaulfuss, G., Sato, K., Lima, P.S., 1999. Paleoproterozoic granulitic belts of the Brazilian southern region (PR-SC). II South American Symposium on Isotope Geology. pp. 291-294. Cordoba, Argentina: Subsecretaría de Minería de la Nación.

Basei, M.A.S., Siga, Jr O., Masquelin, H., Harara, O.M., Reis Neto, J.M., Preciozzi, F., 2000. The Dom Feliciano Belt of Brazil and Uruguay and its Foreland Domain, the Rio de la Plata Craton: framework, tectonic evolution and correlation with similar provinces of Southwestern Africa. In Cordani U. G., et al. eds. Tectonic Evolution of South America. pp. 311-334. Rio de Janeiro, Brazil: Geological Society.

Basei, M.A.S., Frimmel, H.E., Nutman, A.P., Preciozzi, F., Jacob, J., 2005. A connection between the Neoproterozoic Dom Feliciano (Brazil/Uruguay) and Gariep (Namibia/South Africa) orogenic belts - Evidence from a reconnaissance provenance study. Precambrian Res. 139 (3–4), 195–221. https://www.doi.org/10.1016/j.precamres.2005.06.005.

Basei, M.A.S., Campos Neto, M.C., Castro, N.A., Santos, P.R., Siga, Jr. O., Passarelli, C.R., 2006. Mapa Geológico 1:100.000 das Folhas Brusque e Vidal Ramos, SC, Convênio USP-CPRM. XLII Congresso Brasileiro de Geologia, Aracaju, SE.

Basei, M.A.S., Frimmel, H.E., Nutman, A.P., Preciozzi, F., 2008a. West Gondwana amalgamation based on detrital zircon ages from Neoproterozoic Ribeira and Dom Feliciano belts of South America and comparison with coeval sequences from SW Africa. Geol. Soc. Spec. Publ. 294 (1), 239–256. https://www.doi.org/10.1144/SP294.13.

Basei, M.A.S., Grasso, C.B., Vlach, S.R.F., Nutman, A., Siga, Jr. O., Osaki, L.S., 2008b. A-type rift-related granite and the lower cryogenian age for the beginning of the Brusque Belt basin. Proceedings of South American Symposium on Isotope Geology. San Carlos de Bariloche, Argentina.

Basei, M.A.S., Nutman, A., Siga, Jr O., Passarelli, C.R., Drukas, C.O., 2009. The Evolution and Tectonic Setting of the Luis Alves Microplate of Southeastern Brazil: An Exotic Terrane during the Assembly of Western Gondwana. In Gaucher C., et al. eds. Developments in Precambrian Geology. pp. 273-291. Elsevier Doi: 10.1016/S0166-2635(09)01620-X.

Basei, M.A.S., Drukas, C.O., Nutman, A.P., Wemmer, K., Dunyi, L., Santos, P.R., Passarelli, C.R., Campos Neto, M.C., Siga Jr O., Osako, L., 2011a. The Itajaí foreland basin: A tectono-sedimentary record of the Ediacaran period, Southern Brazil. Int. J. Earth Sci., vol. 100, pp. 543–569. https://www.doi.org/10.1007/s00531-010-0604-4.

Basei, M.A.S., Campos Neto, M.C., Castro, N.A., Nutman, A.P., Wemmer, K., Yamamoto, M.T., Hueck, M., Osako, L., Siga, Jr O., Passarelli, C.R., 2011b. Tectonic evolution of the Brusque Group, Dom Feliciano belt, Santa Catarina, Southern Brazil. J. S. Am. Earth Sci., vol. 32, no. 4, pp. 324-350. https://www.doi.org/10.1016/j.jsames.2011.03.016.

Basei, M.A.S., Peel, E., Sánchez, Bettucci L., Preciozzi, F., Nutman, A.P., 2011c. The basement of the Punta del Este Terrane (Uruguay): an African Mesoproterozoic fragment at the eastern border of the South American Río de La Plata craton. Int. J. Earth Sci. 100, 289–304. https://doi.org/10.1007/s00531-010-0623-1.

Basei, M.A.S., Frimmel, H.E., Campos Neto, M.d.C., de Araujo, C.E.G., de Castro, N.A., Passarelli, C.R., 2018. The Tectonic History of the Southern Adamastor Ocean Based on a Correlation of the Kaoko and Dom Feliciano Belts. In Siegesmund S., et al. eds. Geology of Southwest Gondwana. pp. 63-85. 1st ed. Cham: Springer International Publishing Doi: 10.1007/978-3-319-68920-3_3.

Battisti, M.A., Bitencourt, M.F., De Toni, G.B., Nardi, L.V.S., Konopásek, J., 2018. Metavolcanic rocks and orthogneisses from Porongos and Várzea do Capivarita complexes: A case for identification of tectonic interleaving at different crustal levels from structural and geochemical data in southernmost Brazil. J. S. Am. Earth Sci. 88, 253–274. https://doi.org/10.1016/j.jsames.2018.08.009.

Becker, T., Schreiber, U., Kampunzu, A.B., Armstrong, R., 2006. Mesoproterozoic rocks of Namibia and their plate tectonic setting. J. Afr. Earth Sci. 46 (1–2), 112–140. https://doi.org/10.1016/j.jafrearsci.2006.01.015.

Bettucci, L.S., Cosarinsky, M., Ramos, V.A., 2001. Tectonic Setting of the Late Proterozoic Lavalleja Group (Dom Feliciano Belt). Uruguay. Gondwana Res. 4 (3), 395–407. https://doi.org/10.1016/S1342-937X(05)70339-7.

Bial, J., Büttner, S.H., Frei, D., 2015. Formation and emplacement of two contrasting late-Mesoproterozoic magma types in the central Namaqua Metamorphic Complex (South Africa, Namibia): Evidence from geochemistry and geochronology. Lithos 224–225, 272–294. https://doi.org/10.1016/j.lithos.2015.02.021.

Bitencourt, M.F., Nardi, L., 1993. Late- to Post-collisional Brasiliano Magmatism in Southernmost Brazil. Anais da Academia Brasileira de Ciências 65, 3–16.

Bitencourt, M.F., Nardi, L.V.S., 2000. Tectonic setting and sources of magmatism related to the southern Brazilian shear belt. Rev. Brasil. Geocienc. 30 (1), 186–189.
Bybee, G.M., Hayes, B., Owen-Smith, T.M., Lehmann, J., Ashwal, L.D., Brower, A.M., Hill, C.M., Corfu, F., Manga, M., 2019. Proterozoic massif-type anorthosites as the archetypes of long-lived (≥100 Myr) magmatic systems—New evidence from the Kunene Anorthosite Complex (Angola). Precambrian Res. 332, 105393 https://doi.org/10.1016/j.precamres.2019.105393.
Campos, R.S., Philipp, R.P., Massonne, H.-J., Chemale Jr, F., Theye, T., 2011. Petrology and isotope geology of mafic to ultramafic metavolcanic rocks of the Brusque Metamorphic Complex, southern Brazil. Int. Geol. Rev. 54 (6), 686–713. https://doi.org/10.1080/00206814.2011.569393.
Campos, R.S., Philipp, R.P., Massonne, H.-J., Chemale Jr, F., 2012. Early post-collisional Brasiliano magmatism in Botuverá region, Santa Catarina, southern Brazil: Evidence from petrology, geochemistry, isotope geology and geochronology of the diabase and lamprophyre dikes. J. S. Am. Earth Sci. 37, 266–278. https://doi.org/10.1016/j.jsames.2012.02.005.
Cawood, P.A., Hawkesworth, C.J., Dhuime, B., 2012. Detrital zircon record and tectonic setting. Geology 40 (10), 875–878. https://doi.org/10.1130/g32945.1.
Chemale, F., Philipp, R.P., Dussin, I.A., Formoso, M.L.L., Kawashita, K., Berttotti, A.L., 2011. Lu–Hf and U-Pb age determination of Capivarita Anorthosite in the Dom Feliciano Belt. Brazil. Precambrian Res. 186 (1–4), 117–126. https://doi.org/10.1016/j.precamres.2011.01.005.
Chemale, F., Mallmann, G., Bitencourt, M.F., Kawashita, K., 2012. Time constraints on magmatism along the Major Gercino Shear Zone, southern Brazil: Implications for West Gondwana reconstruction. Gondwana Res. 22 (1), 184–199. https://doi.org/10.1016/j.gr.2011.08.018.
Clifford, T.N., Barton, E.S., Stern, R.A., Duchesne, J.-C., 2004. U-Pb Zircon Calendar for Namaquan (Grenville) Crustal Events in the Granulite-facies Terrane of the O'okiep Copper District of South Africa. J. Petrol. 45 (4), 669–691. https://doi.org/10.1093/petrology/egg097.
Condie, K.C., 2016. Chapter 3 - Tectonic Settings. In: Condie, K.C. (Ed.), Earth as an Evolving Planetary System (Third Edition). Academic Press, pp. 43–88. https://doi.org/10.1016/B978-0-12-803689-1.00003-1.
De Toni, G.B., Bitencourt, M.F., Nardi, L.V.S., Florisbal, L.M., Almeida, B.S., Geraldes, M., 2020a. Dom Feliciano Belt orogenic cycle tracked by its pre-collisional magmatism: The Tonian (ca. 800 Ma) Porto Belo Complex and its correlations in southern Brazil and Uruguay. Precambrian Res. 342, 105702 https://doi.org/10.1016/j.precamres.2020.105702.
De Toni, G.B., Bitencourt, M.F., Konopásek, J., Martini, A., Andrade, P.H.S., Florisbal, L.M., Campos, R.S., 2020b. Transpressive strain partitioning between the Major Gercino Shear Zone and the Tijucas Fold Belt, Dom Feliciano Belt, Santa Catarina, southern Brazil. J. Struct. Geol. 136, 104058 https://doi.org/10.1016/j.jsg.2020.104058.
Dickinson, W.R., Gehrels, G.E., 2009. Use of U-Pb ages of detrital zircons to infer maximum depositional ages of strata: A test against a Colorado Plateau Mesozoic database. Earth Planet. Sci. Lett. 288 (1–2), 115–125. https://doi.org/10.1016/j.epsl.2009.09.013.
Drüppel, K., Littmann, S., Romer, R.L., Okrusch, M., 2007. Petrology and isotope geochemistry of the Mesoproterozoic anorthosite and related rocks of the Kunene Intrusive Complex. NW Namibia. Precambrian Res. 156 (1–2), 1–31. https://doi.org/10.1016/j.precamres.2007.02.005.
Evans, D.A.D., 2009. The palaeomagnetically viable, long-lived and all-inclusive Rodinia supercontinent reconstruction. Geol. Soc. Spec. Publ. 327 (1), 371. https://doi.org/10.1144/SP327.16.
Florisbal, L.M., Bitencourt, M.F., Nardi, L.V.S., Conceição, R.V., 2009. Early post-collisional granitic and coeval mafic magmatism of medium- to high-K tholeiitic affinity within the Neoproterozoic Southern Brazilian Shear Belt. Precambrian Res. 175 (1–4), 135–148. https://doi.org/10.1016/j.precamres.2009.09.003.
Florisbal, L.M., Bitencourt, M.F., Janasi, V.d.A., Nardi, L.V.S., Heaman, L.M., 2012a. Petrogenesis of syntectonic granites emplaced at the transition from thrusting to transcurrent tectonics in post-collisional setting: Whole-rock and Sr–Nd–Pb isotope geochemistry in the Neoproterozoic Quatro Ilhas and Mariscal Granites, Southern Brazil. Lithos, vol. 153, pp. 53-71. Doi: 10.1016/j.lithos.2012.04.031.
Florisbal, L.M., de Assis Janasi, V., Bitencourt, M.F., Heaman, L.M., 2012b. Space–time relation of post-collisional granitic magmatism in Santa Catarina, southern Brazil: U-Pb LA-MC-ICP-MS zircon geochronology of coeval mafic–felsic magmatism related to the Major Gercino Shear Zone. Precambrian Res. 216–219, 132–151. https://doi.org/10.1016/j.precamres.2012.06.015.
Foster, D.A., Goscombe, B.D., Newstead, B., Mapani, B., Mueller, P.A., Gregory, L.C., Muvangua, E., 2015. U-Pb age and Lu–Hf isotopic data of detrital zircons from the Neoproterozoic Damara Sequence: Implications for Congo and Kalahari before Gondwana. Gondwana Res. 28 (1), 179–190. https://doi.org/10.1016/j.gr.2014.04.011.
Frantz, J., McNaughton, N.J., Marques, J., Hartmann, L.A., Botelho, N., Caravaca, G., 2003. Shrimp U-Pb zircon ages of granitoids from southernmost Brazil: constraints on the temporal evolution on the Dorsal do Canguçu transcurrent shear zone and the eastern Dom Feliciano Belt. IV South American Symposium on Isotope Geology, pp. 174-177.
Frimmel, H.E., Hartnady, C.J.H., Koller, F., 1996. Geochemistry and tectonic setting of magmatic units in the Pan-African Gariep Belt. Namibia. Chem. Geol. 130 (1–2), 101–121. https://doi.org/10.1016/0009-2541(95)00188-3.
Frimmel, H.E., Zartman, R.E., Späth, A., 2001. The Richtersveld Igneous Complex, South Africa: U-Pb Zircon and Geochemical Evidence for the Beginning of Neoproterozoic Continental Breakup. J. Geol. 109 (4), 493–508. https://doi.org/10.1086/320795.
Frimmel, H.E., Fölling, P.G., 2004. Late Vendian Closure of the Adamastor Ocean: Timing of Tectonic Inversion and Syn-orogenic Sedimentation in the Gariep Basin. Gondwana Res. 7 (3), 685–699. https://doi.org/10.1016/S1342-937X(05)71056-X.
Frimmel, H.E., Basei, M.A.S., Gaucher, C., 2011. Neoproterozoic geodynamic evolution of SW-Gondwana: a southern African perspective. Int. J. Earth Sci. 100, 323–354. https://doi.org/10.1086/320795.
Frimmel, H.E., 2018. The Gariep Belt. In: Siegesmund, S. (Ed.), Geology of Southwest Gondwana, 1st ed. Springer International Publishing, Cham, pp. 353–386.
Gaucher, C., Frei, R., Chemale Jr, F., Frei, D., Bossi, J., Martínez, G., Chiglino, L., Cernuschi, F., 2011. Mesoproterozoic evolution of the Río de la Plata Craton in Uruguay: at the heart of Rodinia? Int. J. Earth Sci. 100 (2), 273–288. https://doi.org/10.1007/s00531-010-0562-x.
Goscombe, B., Hand, M., Gray, D., Mawby, J.O., 2003a. The Metamorphic Architecture of a Transpressional Orogen: the Kaoko Belt. Namibia. J. Petrol. 44 (4), 679–711. https://doi.org/10.1093/petrology/44.4.679.
Goscombe, B., Hand, M., Gray, D., 2003b. Structure of the Kaoko Belt, Namibia: progressive evolution of a classic transpressional orogen. J. Struct. Geol. 25 (7), 1049–1081. https://doi.org/10.1016/S0191-8141(02)00150-5.
Goscombe, B., Gray, D., Armstrong, R., Foster, D.A., Vogl, J., 2005a. Event geochronology of the Pan-African Kaoko Belt. Namibia. Precambrian Res. 140 (3–4), 103.e1–103.e41. https://doi.org/10.1016/j.precamres.2005.07.003.
Goscombe, B., Gray, D., Hand, M., 2005b. Extrusional Tectonics in the Core of a Transpressional Orogen; the Kaoko Belt. Namibia. J. Petrol. 46 (6), 1203–1241. https://doi.org/10.1093/petrology/egi014.
Gray, D.R., Foster, D.A., Meert, J.G., Goscombe, B.D., Armstrong, R., Trouw, R.A.J., Passchier, C.W., 2008. A Damara Orogen perspective on the assembly of southwestern Gondwana. In: Pankhurst, R.J. (Ed.), West Gondwana: Pre-Cenozoic Correlations Across the South Atlantic Region. Geological Society Special Publications, London, pp. 257–278. Doi: 10.1144/SP294.14.
Gross, A.O.M.S., Droop, G.T.R., Porcher, C.C., Fernandes, L.A.D., 2009. Petrology and thermobarometry of mafic granulites and migmatites from the Chafalote Metamorphic Suite: New insights into the Neoproterozoic P-T evolution of the Uruguayan—Sul-Rio-Grandense shield. Precambrian Res. 170 (3–4), 157–174. https://doi.org/10.1016/j.precamres.2009.01.011.
Gruber, L., Porcher, C., Lenz, C., Fernandes, L., 2011. Proveniência de metassedimentos das sequências Arroio Areião, Cerro Cambará e Quartzo Milonitos no Complexo Metamórfico Porongos, Santana da Boa Vista. RS. Pesquisas em Geociencias 38 (3), 205–224. https://doi.org/10.22456/1807-9806.35157.
Gruber, L., Porcher, C.C., Koester, E., Bertotti, A.L., Lenz, C., Fernandes, L.A.D., Remus, M.V.D., 2016. Isotope geochemistry and geochronology of syn-depositional volcanism in Porongos Metamorphic Complex, Santana da Boa Vista Antiform, Dom Feliciano Belt, Brazil: Onset of an 800 Ma continental arc. J. Sediment. Environ. 1 (2), 196–215. https://doi.org/10.12957/jse.2016.22722.
Guadagnin, F., Chemale Jr, F., Dussin, I.A., Jelinek, A.R., dos Santos, M.N., Borba, M.L., Justino, D., Bertotti, A.L., Alessandretti, L., 2010. Depositional age and provenance of the Itajaí Basin, Santa Catarina State, Brazil: Implications for SW Gondwana correlation. Precambrian Res. 180 (3–4), 156–182. https://doi.org/10.1016/j.precamres.2010.04.002.
Hartmann, L.A., Basei, M.A.S., Simas, M.W., 1999. Geochemistry of the Lower Proterozoic granulite-facies Grant syenite gneiss, Barra Velha, Santa Catarina State, southern Brazil. Pesquisas em Geociencias 25, 3–9.
Hartmann, L.A., Santos, J.O.S., McNaughton, N.J., Vasconcellos, M.A.Z., da Silva, L.C., 2000. Ion microprobe (SHRIMP) dates complex granulite from Santa Catarina, southern Brazil. Anais da Academia Brasileira de Ciencias 72 (4), 559–572. https://doi.org/10.1590/S0001-37652000000400007.
Hartmann, L.A., Bitencourt, M.F., Santos, J.O.S., McNaughton, N.J., Rivera, C.B., Betiollo, L., 2003. Prolonged Paleoproterozoic magmatic participation in the Neoproterozoic Dom Feliciano belt, Santa Catarina, Brazil, based on zircon U-Pb SHRIMP geochronology. J. S. Am. Earth Sci. 16 (6), 477–492. https://doi.org/10.1016/j.jsames.2003.04.001.
Hartmann, L.A., Savian, J.F., Lopes, W.R., 2015. Airborne geophysical characterization of geotectonic relationships in the southern Ribeira Belt, Luís Alves Craton, and northern Dom Feliciano Belt. Brazilian Shield. Int. Geol. Rev. 58 (4), 471–488. https://doi.org/10.1080/00206814.2015.1089424.
Heine, C., Zoethout, J., Müller, R.D., 2013. Kinematics of the South Atlantic rift. Solid Earth 4 (2), 215–253. https://doi.org/10.5194/se-4-215-2013.
Hoffman, P.F., Halverson, G.P., 2008. Otavi Group of the western Northern Platform, the Eastern Kaoko Zone and the western Northern Margin Zone. In: Miller, R.M. (Ed.), The Geology of Namibia. Geological Survey Namibia, Namibia, pp. 69–136.
Höfig, D.F., Marques, J.C., Basei, M.A.S., Giusti, R.O., Kohlrausch, C., Frantz, J.C., 2018. Detrital zircon geochronology (U-Pb LA-ICP-MS) of syn-orogenic basins in SW Gondwana: New insights into the Cryogenian-Ediacaran of Porongos Complex, Dom Feliciano Belt, southern Brazil. Precambrian Res. 306, 189–208. https://doi.org/10.1016/j.precamres.2017.12.031.
Hofmann, M., Linnemann, U., Hoffmann, K.-H., Gerdes, A., Eckelmann, K., Gärtner, A., 2014. The Namuskluft and Dreigratberg sections in southern Namibia (Kalahari Craton, Gariep Belt): a geological history of Neoproterozoic rifting and recycling of cratonic crust during the dispersal of Rodinia until the amalgamation of Gondwana. Int. J. Earth Sci. 103 (5), 1187–1202. https://doi.org/10.1007/s00531-013-0949-6.
Hofmann, M., Linnemann, U., Hoffmann, K.-H., Germs, G., Gerdes, A., Marko, L., Eckelmann, K., Gärtner, A., Krause, R., 2015. The four Neoproterozoic glaciations of southern Namibia and their detrital zircon record: The fingerprints of four crustal growth events during two supercontinent cycles. Precambrian Res. 259, 176–188. https://doi.org/10.1016/j.precamres.2014.07.021.
Hueck, M., Basei, M.A.S., Wemmer, K., Oriolo, S., Heidelbach, F., Siegesmund, S., 2018a. Evolution of the Major Gercino Shear Zone in the Dom Feliciano Belt, South Brazil,

and implications for the assembly of southwestern Gondwana. Int. J. Earth Sci. 108 (2), 403–425. https://doi.org/10.1007/s00531-018-1660-4.
Hueck, M., Oyhantçabal, P., Basei, M., Siegesmund, S., 2018b. The Dom Feliciano Belt in Southern Brazil and Uruquay. In: Siegesmund, S. (Ed.), Geology of Southwest Gondwana, 1st ed. Springer International Publishing, Cham, pp. 267–302.
Hueck, M., Basei, M.A.S., Castro, N.A.d., 2019. Tracking the sources and the evolution of the late Neoproterozoic granitic intrusions in the Brusque Group, Dom Feliciano Belt, South Brazil: LA-ICP-MS and SHRIMP geochronology coupled to Hf isotopic analysis. Precambrian Res. 338, 105566 https://doi.org/10.1016/j.precamres.2019.105566.
Johansson, Å., 2014. From Rodinia to Gondwana with the 'SAMBA' model—A distant view from Baltica towards Amazonia and beyond. Precambrian Res. 244, 226–235. https://doi.org/10.1016/j.precamres.2013.10.012.
Koester, E., Porcher, C.C., Pimentel, M.M., Fernandes, L.A.D., Vignol-Lelarge, M.L., Oliveira, L.D., Ramos, R.C., 2016. Further evidence of 777 Ma subduction-related continental arc magmatism in Eastern Dom Feliciano Belt, southern Brazil: The Chácara das Pedras Orthogneiss. J. S. Am. Earth Sci. 68, 155–166. https://www.doi.org/10.1016/j.jsames.2015.12.006.
Konopásek, J., Kosler, J., Tajcmanova, L., Ulrich, S., Kitt, S., 2008. Neoproterozoic igneous complex emplaced along major tectonic boundary in the Kaoko Belt (NW Namibia): ion probe and LA-ICP-MS dating of magmatic and metamorphic zircons. J. Geol. Soc. London 165 (1), 153–165.
Konopásek, J., Košler, J., Sláma, J., Janoušek, V., 2014. Timing and sources of pre-collisional Neoproterozoic sedimentation along the SW margin of the Congo Craton (Kaoko Belt, NW Namibia). Gondwana Res. 26 (1), 386–401. https://www.doi.org/10.1016/j.gr.2013.06.021.
Konopásek, J., Sláma, J., Košler, J., 2016. Linking the basement geology along the Africa-South America coasts in the South Atlantic. Precambrian Res. 280, 221–230. https://www.doi.org/10.1016/j.precamres.2016.05.011.
Konopásek, J., Hoffmann, K.-H., Sláma, J., Košler, J., 2017. The onset of flysch sedimentation in the Kaoko Belt (NW Namibia) – Implications for the pre-collisional evolution of the Kaoko-Dom Feliciano–Gariep orogen. Precambrian Res. 298, 220–234. https://doi.org/10.1016/j.precamres.2017.06.017.
Konopásek, J., Janoušek, V., Oyhantçabal, P., Sláma, J., Ulrich, S., 2018. Did the circum-Rodinia subduction trigger the Neoproterozoic rifting along the Congo-Kalahari Craton margin? Int. J. Earth Sci. 107 (5), 1859–1894. https://www.doi.org/10.1007/s00531-017-1576-4.
Konopásek, J., Cavalcante, C., Fossen, H., Janoušek, V., 2020. Adamastor – an ocean that never existed? Earth-Sci. Rev. 205, 103201 https://doi.org/10.1016/j.earscirev.2020.103201.
Kröner, A., Rojas-Agramonte, Y., Hegner, E., Hoffmann, K.H., Wingate, M.T.D., 2010. SHRIMP zircon dating and Nd isotopic systematics of Palaeoproterozoic migmatitic orthogneisses in the Epupa Metamorphic Complex of northwestern Namibia. Precambrian Res. 183 (1), 50–69. https://doi.org/10.1016/j.precamres.2010.06.018.
Kröner, A., Rojas-Agramonte, Y., Wong, J., Wilde, S.A., 2015. Zircon reconnaissance dating of Proterozoic gneisses along the Kunene River of northwestern Namibia. Tectonophysics 662, 125–139. https://doi.org/10.1016/j.tecto.2015.04.020.
Kröner, A., Rojas-Agramonte, Y., 2017. Mesoproterozoic (Grenville-age) granitoids and supracrustal rocks in Kaokoland, northwestern Namibia. Precambrian Res. 298, 572–592. https://doi.org/10.1016/j.precamres.2017.07.008.
Kröner, S., Konopásek, J., Kröner, A., Passchier, C.W., Poller, U., Wingate, M.T.D., Hofmann, K.H., 2004. U-Pb and Pb-Pb zircon ages for metamorphic rocks in the Kaoko Belt of Northwestern Namibia: A Palaeo- to Mesoproterozoic basement reworked during the Pan-African orogeny. S. Afr. J. Geol. 107 (3), 455–476. https://www.doi.org/10.2113/107.3.455.
Lara, P., Oyhantçabal, P., Belousova, E., 2020. Two distinct crustal sources for Late Neoproterozoic granitic magmatism across the Sierra Ballena Shear Zone, Dom Feliciano Belt, Uruguay: Whole-rock geochemistry, zircon geochronology and Sr-Nd-Hf isotope evidence. Precambrian Res. 341, 105625 https://doi.org/10.1016/j.precamres.2020.105625.
Lehmann, J., Bybee, G.M., Hayes, B., Owen-Smith, T.M., Belyanin, G., 2020. Emplacement of the giant Kunene AMCG complex into a contractional ductile shear zone and implications for the Mesoproterozoic tectonic evolution of SW Angola. Int. J. Earth Sci. 109 (4), 1463–1485. https://doi.org/10.1007/s00531-020-01837-5.
Lenz, C., Fernandes, L.A.D., McNaughton, N.J., Porcher, C.C., Masquelin, H., 2011. U-Pb SHRIMP ages for the Cerro Bori Orthogneisses, Dom Feliciano Belt in Uruguay: Evidences of a ~800Ma magmatic and ~650Ma metamorphic event. Precambrian Res. 185 (3), 149–163. https://doi.org/10.1016/j.precamres.2011.01.007.
Lenz, C., Porcher, C., Fernandes, L., Masquelin, H., Koester, E., Conceição, R., 2013. Geochemistry of the Neoproterozoic (800–767 Ma) Cerro Bori orthogneisses, Dom Feliciano Belt in Uruguay: tectonic evolution of an ancient continental arc. Mineral. Petrol. 107, 785–806. https://www.doi.org/10.1007/s00710-012-0244-4.
Li, Z.-X., Bogdanova, S.V., Collins, A.S., Davidson, A., De Waele, B., Ernst, R.E., Fitzsimons, I.C.W., Fuck, R.A., Gladkochub, D.P., Jacobs, J., Karlstrom, K.E., Lu, S., Natapov, L.M., Pease, V., Pisarevsky, S.A., Thrane, K., Vernikovsky, V., 2008. Assembly, configuration, and break-up history of Rodinia: A synthesis. Precambrian Res. 160 (1), 179–210. https://doi.org/10.1016/j.precamres.2007.04.021.
Li, Z.-X., Evans, D.A.D., Halverson, G.P., 2013. Neoproterozoic glaciations in a revised global palaeogeography from the breakup of Rodinia to the assembly of Gondwanaland. Sediment. Geol. 294, 219–232. https://doi.org/10.1016/j.sedgeo.2013.05.016.
Luft, J.L., Chemale Jr, F., Armstrong, R., 2011. Evidence of 1.7- to 1.8-Ga Collisional Arc in the Kaoko Belt. NW Namibia. Int. J. Earth Sci. 100, 305–321. https://www.doi.org/10.1007/s00531-010-0591-5.
Macey, P.H., Abrahams, Y., Miller, J.A., 2018. Lithostratigraphy of the Mesoproterozoic Stolzenfels Enderbite (Komsberg Suite), South Africa and Namibia. S. Afr. J. Geol. 121 (2), 217–226. https://www.doi.org/10.25131/sajg.121.0016.
Mallmann, G., Chemale Jr, F., Ávila, J.N., Kawashita, K., Armstrong, R.A., 2007. Isotope geochemistry and geochronology of the Nico Pérez Terrane, Rio de la Plata Craton. Uruguay. Gondwana Res. 12 (4), 489–508. https://doi.org/10.1016/j.gr.2007.01.002.
Martil, M.M.D., Bitencourt, M.F., Nardi, L.V.S., Koester, E., Pimentel, M.M., 2017. Pre-collisional, Tonian (ca. 790 Ma) continental arc magmatism in southern Mantiqueira Province, Brazil: Geochemical and isotopic constraints from the Várzea do Capivarita Complex. Lithos 274–275, 39–52. https://doi.org/10.1016/j.lithos.2016.11.011.
Martini, A., Bitencourt, M.F., Weinberg, R.F., De Toni, G.B., Lauro, V.S.N., 2019. From migmatite to magma - crustal melting and generation of granite in the Camboriú Complex, south Brazil. Lithos 340–341, 270–286. https://www.doi.org/10.1016/j.lithos.2019.05.017.
Masquelin, H., Fernandes, L., Lenz, C., Porcher, C.C., McNaughton, N.J., 2012. The Cerro Olivo Complex: A pre-collisional Neoproterozoic magmatic arc in Eastern Uruguay. Int. Geol. Rev. 54, 1161–1183. https://www.doi.org/10.1080/00206814.2011.626597.
McCourt, S., Armstrong, R., Jelsma, H., Mapeo, R., 2013. New U-Pb SHRIMP ages from the Lubango region, SW Angola: Insights into the Palaeoproterozoic evolution of the Angolan Shield, southern Congo Craton. Africa. Geol. Soc. Spec. Publ. 170 (2), 353–363. https://www.doi.org/10.1144/jgs2012-059.
Merdith, A.S., Collins, A.S., Williams, S.E., Pisarevsky, S., Foden, J.D., Archibald, D.B., Blades, M.L., Alessio, B.L., Armistead, S., Plavsa, D., Clark, C., Müller, D.R., 2017a. A Full-Plate Global Reconstruction of the Neoproterozoic. Gondwana Res. 50, 84–134. https://www.doi.org/10.1016/j.gr.2017.04.001.
Merdith, A.S., Williams, S.E., Müller, R.D., Collins, A.S., 2017b. Kinematic constraints on the Rodinia to Gondwana transition. Precambrian Res. 299, 132–150. https://doi.org/10.1016/j.precamres.2017.07.013.
Miller, R.M., 2012. Review of Mesoproterozoic magmatism, sedimentation and terrane amalgamation in southwestern Africa. S. Afr. J. Geol. 115 (4), 417–448. https://www.doi.org/10.2113/gssajg.115.4.417.
Oriolo, S., Oyhantçabal, P., Basei, M.A.S., Wemmer, K., Siegesmund, S., 2016. The Nico Pérez Terrane (Uruguay): From Archean crustal growth and connections with the Congo Craton to late Neoproterozoic accretion to the Río de la Plata Craton. Precambrian Res. 280, 147–160. https://doi.org/10.1016/j.precamres.2016.04.014.
Oriolo, S., Oyhantçabal, P., Konopásek, J., Basei, M.A.S., Frei, R., Sláma, J., Wemmer, K., Siegesmund, S., 2019. Late Paleoproterozoic and Mesoproterozoic magmatism of the Nico Pérez Terrane (Uruguay): Tightening up correlations in southwestern Gondwana. Precambrian Res. 327, 296–313. https://doi.org/10.1016/j.precamres.2019.04.012.
Oyhantçabal, P., Siegesmund, S., Wemmer, K., Frei, R., Layer, P., 2007. Post-collisional transition from calc-alkaline to alkaline magmatism during transcurrent deformation in the southernmost Dom Feliciano Belt (Braziliano–Pan-African, Uruguay). Lithos 98 (1–4), 141–159. https://doi.org/10.1016/j.lithos.2007.03.001.
Oyhantçabal, P., Siegesmund, S., Wemmer, K., Presnyakov, S., Layer, P., 2009. Geochronological constraints on the evolution of the southern Dom Feliciano Belt (Uruguay). J. Geol. Soc. 166 (6), 1075–1084. https://www.doi.org/10.1144/0016-76492008-122.
Oyhantçabal, P., Siegesmund, S., Wemmer, K., Passchier, C.W., 2011a. The transpressional connection between Dom Feliciano and Kaoko Belts at 580–550 Ma. Int. J. Earth Sci. 100, 379–390. https://www.doi.org/10.1007/s00531-010-0577-3.
Oyhantçabal, P., Siegesmund, S., Wemmer, K., 2011b. The Río de la Plata Craton: a review of units, boundaries, ages and isotopic signature. Int. J. Earth Sci. 100 (2), 201–220. https://www.doi.org/10.1007/s00531-010-0580-8.
Oyhantçabal, P., Oriolo, S., Philipp, R.P., Wemmer, K., Siegesmund, S., 2018. The Nico Pérez Terrane of Uruguay and Southeastern Brazil. In: Siegesmund, S. (Ed.), Geology of Southwest Gondwana. Springer International Publishing 10.1007/978-3-319-68920-3_7, Cham, pp. 161–188.
Passarelli, C.R., Basei, M.A.S., Siga, O., Harara, O.M.M., 2018. The Luis Alves and Curitiba Terranes: Continental Fragments in the Adamastor Ocean. In: Siegesmund, S. (Ed.), Geology of Southwest Gondwana. Springer International Publishing, Cham, pp. 189–215 https://www.doi.org/10.1007/978-3-319-68920-3_8.
Pertille, J., Hartmann, L.A., Philipp, R.P., 2015a. Zircon U-Pb age constraints on the Paleoproterozoic sedimentary basement of the Ediacaran Porongos Group, Sul-Riograndense Shield, southern Brazil. J. S. Am. Earth Sci. 63, 334–345. https://doi.org/10.1016/j.jsames.2015.08.005.
Pertille, J., Hartmann, L.A., Philipp, R.P., Petry, T.S., de Carvalho Lana, C., 2015b. Origin of the Ediacaran Porongos Group, Dom Feliciano Belt, southern Brazilian Shield, with emphasis on whole rock and detrital zircon geochemistry and U-Pb, Lu–Hf isotopes. J. S. Am. Earth Sci. 64, 69–93. https://www.doi.org/10.1016/j.jsames.2015.09.001.
Pertille, J., Hartmann, L.A., Santos, J.O.S., McNaughton, N.J., Armstrong, R., 2017. Reconstructing the Cryogenian-Ediacaran evolution of the Porongos fold and thrust belt, Southern Brasiliano Orogen, based on Zircon U-Pb–Hf–O isotopes. Int. Geol. Rev. 59 (12), 1532–1560. https://www.doi.org/10.1080/00206814.2017.1285257.
Philipp, R.P., Machado, R., 2005. The Neoproterozoic to Cambrian granitic magmatism of the Pelotas Batholith, Southern Brazil. J. S. Am. Earth Sci. 19, 461–478.
Philipp, R.P., Massonne, H.-J., de Campos, R.S., 2013. Peraluminous leucogranites of the Cordilheira Suite: A record of Neoproterozoic collision and the generation of the Pelotas Batholith, Dom Feliciano Belt, Southern Brazil. J. S. Am. Earth Sci. 43, 8–24. https://www.doi.org/10.1016/j.jsames.2012.10.006.
Philipp, R.P., Pimentel, M.M., Chemale Jr, F., 2016. Tectonic evolution of the Dom Feliciano Belt in Southern Brazil: Geological relationships and U-Pb geochronology.

Braz. J. Geol. 46, 83–104. https://www.doi.org/10.1590/2317-488920162015001 6.
Porada, H., 1989. Pan-African rifting and orogenesis in southern to equatorial Africa and eastern Brazil. Precambrian Res. 44 (2), 103–136. https://doi.org/10.1016/0301-9268(89)90078-8.
Rapela, C.W., Fanning, C.M., Casquet, C., Pankhurst, R.J., Spalletti, L., Poiré, D., Baldo, E.G., 2011. The Rio de la Plata craton and the adjoining Pan-African/brasiliano terranes: Their origins and incorporation into south-west Gondwana. Gondwana Res. 20 (4), 673–690. https://doi.org/10.1016/j.gr.2011.05.001.
Saalmann, K., Remus, M.V.D., Hartmann, L.A., 2006. Structural evolution and tectonic setting of the Porongos belt, southern Brazil. Geol. Mag. 143 (1), 59–88. https://www.doi.org/10.1017/S0016756805001433.
Saalmann, K., Gerdes, A., Lahaye, Y., Hartmann, L., Remus, M., Läufer, A., 2011. Multiple accretion at the eastern margin of the Rio de la Plata craton: the prolonged Brasiliano orogeny in southernmost Brazil. Int. J. Earth Sci. 100, 355–378. https://www.doi.org/10.1007/s00531-010-0564-8.
Sánchez-Bettucci, L., Oyhantçabal, P., Loureiro, J., Ramos, V.A., Preciozzi, F., Basei, M.A. S., 2004. Mineralizations of the Lavalleja Group (Uruguay), a Probable Neoproterozoic Volcano-sedimentary Sequence. Gondwana Res. 7 (3), 745–751. https://www.doi.org/10.1016/S1342-937X(05)71060-1.
Seth, B., Kröner, A., Mezger, K., Nemchin, A.A., Pidgeon, R.T., Okrusch, M., 1998. Archaean to Neoproterozoic magmatic events in the Kaoko belt of NW Namibia and their geodynamic significance. Precambrian Res. 92 (4), 341–363. https://doi.org/10.1016/S0301-9268(98)00086-2.
Seth, B., Armstrong, R.A., Brandt, S., Villa, I.M., Kramers, J.D., 2003. Mesoproterozoic U-Pb and Pb–Pb ages of granulites in NW Namibia: reconstructing a complete orogenic cycle. Precambrian Res. 126 (1–2), 147–168. https://doi.org/10.1016/S0301-9268(03)00193-1.
Silva, L.C., Hartmann, L.A., McNaughton, N.J., Fletcher, I., 2000. Zircon U-Pb SHRIMP dating of a Neoproterozoic overprint in Paleoproterozoic granitic-gneissic terranes, southern Brazil. Am. Mineral. 85 (5–6), 649–667. https://www.doi.org/10.2138/am-2000-5-602.
Silva, L.C., McNaughton, N.J., Fletcher, I.R., 2005. SHRIMP U-Pb zircon geochronology of Neoproterozoic crustal granitoids (Southern Brazil): A case for discrimination of emplacement and inherited ages. Lithos 82 (3–4), 503–525. https://doi.org/10.1016/j.lithos.2004.09.029.
Vermeesch, P., 2012. On the visualisation of detrital age distributions. Chem. Geol. 312–313, 190–194. https://doi.org/10.1016/j.chemgeo.2012.04.021.
Vermeesch, P., Resentini, A., Garzanti, E., 2016. An R package for statistical provenance analysis. Sediment. Geol. 336, 14–25. https://doi.org/10.1016/j.sedgeo.2016.01.009.
Will, T.M., Gaucher, C., Ling, X.X., Li, X.H., Li, Q.L., Frimmel, H.E., 2019. Neoproterozoic magmatic and metamorphic events in the Cuchilla Dionisio Terrane, Uruguay, and possible correlations across the South Atlantic. Precambrian Res. 320, 303–322. https://doi.org/10.1016/j.precamres.2018.11.004.
Zimmermann, U., 2018. The Provenance of Selected Neoproterozoic to Lower Paleozoic Basin Successions of Southwest Gondwana: A Review and Proposal for Further Research. In: Siegesmund, S. (Ed.), Geology of Southwest Gondwana. Springer International Publishing, Cham, pp. 561–591. https://doi.org/10.1007/978-3-319-68920-3_7.